







A Coupled Hydrological-Hydrodynamic Modelling Approach for Assessing the Impacts of Multiple Natural Flood Management Interventions on Downstream Flooding

Qiuyu Zhu¹ 📵 | Megan Klaar¹ | Thomas Willis^{1,2,3} | Joseph Holden¹

 1 water@leeds, School of Geography, University of Leeds, Leeds, UK 1 School of Geography and the Environment, University of Oxford, Oxford, UK 1 Senvironment Agency, Leeds, UK

Correspondence: Qiuyu Zhu (qiuyu.w.z@gmail.com)

Received: 25 April 2025 | Revised: 20 August 2025 | Accepted: 30 August 2025

Keywords: flood mitigation | flood risk management plans | hydraulic modelling | hydrological modelling | natural flood management | nature-based solutions

ABSTRACT

While natural flood management (NFM) as a flood mitigation strategy is becoming widely used, there remains a lack of evidence regarding the effectiveness of different NFM scenarios under high flow events. To demonstrate how different types and extents of NFM interventions interact to flood peaks at larger catchment scales, combined scenarios of existing NFM interventions and an ideal maximum woodland scenario were modelled in the Upper Aire, northern England, using a coupled model that integrates Spatially Distributed TOPMODEL (SD-TOPMODEL) with a 2D hydrodynamic model (Flood Modeller 2D) at an 81.4 km² catchment. The coupled model exhibited a strong fit with observed data (NSE up to 0.95), effectively capturing flood peaks and peak shapes. Leaky dams were found to be more effective at delaying flood peaks with mean values ranging from 8.6 to 60 min than reducing peak discharge (mean values ranging from 0.53% to 1.84%), though these effects were inversely proportional and influenced by tributary characteristics such as channel gradient. Simulations applying multiple NFM interventions consistently demonstrated positive flood mitigation impacts, including reduced peak discharge up to 2.59% and delayed peaks up to 30 min, while inundation depths reduced by 0.5 m in most areas, with inundation extent reduction at critical points in an urban area. The study demonstrated the utility of the coupled model for evaluating NFM strategies while emphasising the need for further validation and exploration of systematic interventions at larger catchment scales. By providing insights into the interactions between NFM interventions and catchment characteristics, this research contributes to the optimisation of flood risk management strategies and informs future policy development.

1 | Introduction

The number of studies related to nature-based solutions (NBSs) has grown rapidly over the last decade, including a large number of natural flood management (NFM)-related studies (Thaler et al. 2023; Zhu et al. 2024). NFM, as a subset of NBS, attempts to work with natural processes to reduce flood risks (Iacob et al. 2014; Dadson et al. 2017) and currently requires a shift from pursuing localised flood mitigation effects to catchment-wide

flood management strategies (Lane 2017; Wilkinson et al. 2019; Bark et al. 2021; Black et al. 2021; Carter et al. 2024; Lalonde et al. 2024; Zhu et al. 2024). Leaky dams, riparian buffer strips and land and soil management are often utilised as NFM interventions to achieve flood mitigation. Leaky dams reduce flow velocity in the channels and increase upstream and adjacent channel overflow to the floodplain (Kitts 2010; Thomas and Nisbet 2012; Addy and Wilkinson 2019; Grabowski et al. 2019; Hankin et al. 2020; Norbury et al. 2021; Follett and Hankin 2022;

This is an open access article under the terms of the Creative Commons Attribution License, which permits use, distribution and reproduction in any medium, provided the original work is properly cited.

© 2025 The Author(s). Journal of Flood Risk Management published by Chartered Institution of Water and Environmental Management and John Wiley & Sons Ltd.

van Leeuwen et al. 2024). Expandable field storage alongside riparian buffer strips increases surface and subsurface storage capacity with greater surface roughness in the floodplain and offline storage (Metcalfe et al. 2017, 2018; Keys et al. 2018; Hankin et al. 2019; Beven et al. 2022; Lockwood et al. 2022). NFM interventions based on land and soil management can slow the rainfall-runoff response process in the catchment by increasing infiltration rates and soil water storage capacity (Marshall et al. 2014; Dixon et al. 2016; Gao et al. 2016; Bond et al. 2022; Monger et al. 2024; Zhu et al. 2025). Evidence shows that interventions like woodland planting, peatland restoration and soil aeration can reduce overland flow and delay peaks by improving soil water retention and surface roughness (Archer et al. 2013; Gao et al. 2016; Alaoui et al. 2018; Shuttleworth et al. 2019; Bond et al. 2020; Goudarzi et al. 2021, 2024; Zhu et al. 2025). Research suggests that the implementation of multiple NFM interventions in a catchment has the potential to enhance flood mitigation effectiveness; however, the interactions and impacts of different types of interventions remain uncertain (Ramsbottom et al. 2019; Ferreira et al. 2020; Nicholson et al. 2020; Black et al. 2021; Carter et al. 2024; Zhu et al. 2024, 2025). The effectiveness of flood mitigation has not been consistently improved by the deployment of multiple interventions across all study catchments, suggesting that factors such as catchment scale, spatial extent and the location of interventions play a significant role (Dixon et al. 2016; Kay et al. 2019; Barnsley et al. 2021; Black et al. 2021; Kingsbury-Smith et al. 2023). These findings highlight a critical need to better understand the impacts of a network of multiple NFM interventions on flood risks at the catchment scale.

NFM interventions designed to reduce peak flows by altering soil properties and surface roughness properties have been successfully modelled in SD-TOPMODEL (Gao et al. 2016; Bond et al. 2022; Monger et al. 2024; Zhu et al. 2025). A subsequent step entails expanding this modelling framework to include surface structures introduced by NFM interventions within river channels and floodplains (Metcalfe et al. 2017; Hankin et al. 2021; Senior et al. 2022; Barnes et al. 2023; Villamizar et al. 2024). The integration of a coupled hydrological and hydrodynamic model could offer a robust approach for encompassing all types of NFM interventions (Hankin et al. 2019; Ferguson and Fenner 2020). This coupled approach also presents potential benefits for scaling up to larger catchments and enhancing flood-related outputs, including inundation extents and depths (Hill et al. 2023).

Both physical experiments and modelling studies have demonstrated that increasing the number of NFM interventions within small tributaries can enhance peak flow reduction (Thomas and Nisbet 2012; Hankin et al. 2020; Follett et al. 2021, 2024; Follett and Hankin 2022), but their efficacy is constrained by factors such as the location and physical properties of features such as leaky dams, as well as the characteristics of the tributary and its contribution to the overall catchment hydrology (Hankin et al. 2020; Black et al. 2021; Norbury et al. 2021; Follett and Hankin 2022; van Leeuwen et al. 2024). A combination of geometric structure and roughness adjustments has been used to represent leaky dams within stream networks in one-dimensional (1D) and two-dimensional (2D) hydrodynamic models (Addy and Wilkinson 2019; Leakey et al. 2020;

Follett and Hankin 2022; Senior et al. 2022; Barnes et al. 2023; Villamizar et al. 2024). However, uncertainties remain regarding the effectiveness of leaky dams under varying hydrological scenarios, necessitating further investigation. A notable gap in the existing literature is the limited evidence on the combined or cross-scale impacts of leaky dams and other NFM interventions at the catchment scale, particularly, for areas larger than 50 km² (Metcalfe et al. 2017; Barnes et al. 2023; Zhu et al. 2024).

This study aims to evaluate the effectiveness of multiple NFM interventions at a catchment scale larger than 50 km² using a coupled hydrological-hydrodynamic modelling approach. To achieve this, SD-TOPMODEL was coupled with Flood Modeller 2D to simulate responses in an 81.4 km² catchment. This coupled modelling approach enables the simultaneous and independent representation of various NFM intervention types (woodland planting, hedgerow planting, soil aeration, leaky dams and riparian fencing and buffer strips) within a catchment, facilitating the simulation of different intervention combinations and idealised scenarios. It also addresses a key gap in modelling the integrated impacts of multiple NFM interventions at larger catchment scales. As the first coupling of SD-TOPMODEL and Flood Modeller 2D, this study also compares the performance and outputs of the two models to demonstrate the feasibility and reliability of the coupling process, as well as to identify any uncertainties it may introduce. The findings of this study offer novel insights into the variability of NFM intervention effectiveness across tributaries and under different flood event characteristics, as well as the implications for scaling these interventions from tributary to catchment levels. Furthermore, the study explores the interplay between flood peak delay, peak discharge reduction and inundation extent, highlighting limitations at broader scales and emphasising the need for further research to design effective catchment-scale NFM schemes.

2 | Data and Sources

2.1 | Study Sites

The Upper Aire catchment draining to Gargrave covers 81.4 km² with elevation ranging from 572 to 105 m (Figure 1). The mean annual precipitation at Malham Tarn station (54°06'00" N, 02°09'49" W) for 1991-2020 was 1587 mm, with monthly mean totals ranging from 90.9 to 181.3 mm, with typically less rainfall in spring and summer and more in autumn and winter (Met Office 2024). The headwaters are formed of many small, dendritic streams. The dominant soils are characterised by very shallow or slowly permeable loamy soils (LandIS 2016). The predominant land cover in the catchment is improved grassland, followed by calcareous grassland, acid grassland, heather grassland and woodland. The woodland consists of both broadleaf and coniferous woodland, which contributes to instream wood inputs and the source of materials for artificial woody dams in the catchment (Grabowski et al. 2019; Hankin et al. 2020). Several streams within the catchment are documented to have leaky dam installations to slow the overland flows (Yorkshire Wildlife Trust 2022). For modelling purposes, four sub-catchments were delineated based on the locations of these leaky dams (Figure 1). The sub-catchments extend from headwaters to the seventh or eighth stream order (Strahler 1957) at their confluences. Each

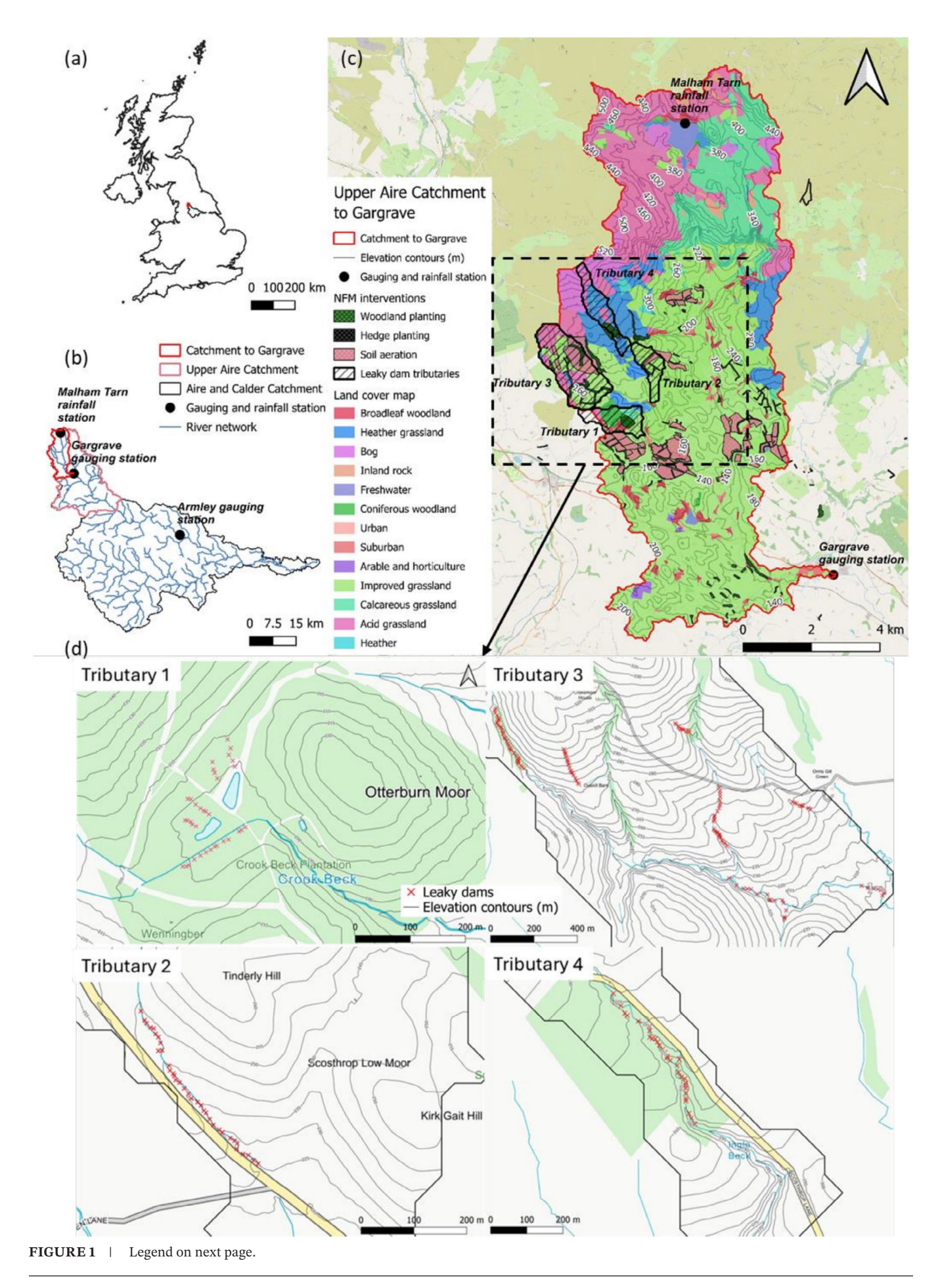


FIGURE 1 | Study site: (a) location of study catchment in the United Kingdom; (b) Aire and Calder catchment; (c) study area upstream of Gargrave gauging station, Upper Aire Catchment, North Yorkshire, UK. Location of NFM interventions in the study area and the Environment Agency operated rainfall station and gauging stations. The inset (d) shows the location of four modelled streams with leaky dams in the research catchment.

TABLE 1 | Leaky dam tributary catchment characteristics.

Tributary	Highest elevation (m)	Lowest elevation (m)	Catchment area (km²)	Average channel gradient (m/m)	Number of leaky dams applied	Number of points used for coupling	Final stream order
1	274	159	1.13	0.037	35	4	8
2	302	181	0.79	0.024	35	2	7
3	379	201	2.89	0.034	125	4	7
4	513	247	1.16	0.023	33	1	7

sub-catchment joins the main channel of the River Aire, providing a logical framework for coupling steps in the modelling process. To understand the impacts of leaky dams on overland flow, the coupled model was individually simulated on the four sub-catchments. In addition to leaky dams, woodland planting, hedge planting and soil aeration, multiple riparian fencing and buffer strips have been applied in the catchment as NFM interventions for flood mitigation since 2017 (Yorkshire Wildlife Trust 2022) (Figure 1).

2.2 | Data Sources

Elevation data for the catchments were obtained from the Ordnance Survey Terrain 5m digital terrain model (DTM) (Ordnance Survey 2022). The stream catchment area (Table 1) and boundaries were obtained from the Flood Estimation Handbook (FEH) (Rowland et al. 2017). The number and locations of leaky dams applied in each tributary catchment were determined using data provided by Yorkshire Wildlife Trust, relating to locations where dams have already been installed as part of NFM interventions. For rainfall data, the study used 15-min measured precipitation (mm) from the Malham Tarn station, which is situated near a natural lake at the headwaters of River Aire (station number 73422; Figure 1b) (Environment Agency 2022). The 15-min observed river flow data (m³/s) was used for model calibration and validation from the Gargrave station (53°58′54" N, 02°05′49" W, station number F1508) during 2012-2022 (Figure 1) (Environment Agency 2022). Gargrave gauging station is located on the main channel of the River Aire, with a stage datum of 104.8 mAOD.

In this study, land cover inputs derived from the UKCEH (2015) land cover map served as the baseline layer for all coupled model simulations. Based on the land cover map, multiple NFM interventions known to have been applied in the study catchment were selected, including woodland planting, hedge planting, soil aeration, leaky dams and riparian buffer strips (Figure 1c). To investigate the impacts that potential NFM opportunities and expanded NFM implementation within the catchment may have on flood mitigation, the study generated a potential

woodland map (Figure SI.5) by incorporating the Environment Agency's Working with Natural Processes (WWNP) dataset (Environment Agency 2024a). It provided all potential locations within the catchment which could be covered by woodland (66.86% of the catchment area).

2.3 | High Flow Events

To model the potential impacts of NFM interventions during different characteristic flood events, a range of high flow periods was determined from rainfall and discharge data. These high-flow periods were selected to represent flood events for modelling before and after NFM implementation or other scenarios. High flow events were permitted to be single or multipeaked for diversity. Discrete events were identified from observed river flow and precipitation time series using a similar rules-based methodology to Deasy et al. (2009) and van Leeuwen et al. (2024). Peak over threshold (POT) and annual maximum (AMAX) series of discharge data (National River Flow Archive 2024) from an Environment Agency maintained flow gauging station at Armley gauging station (in the city of Leeds; Figure 1b) on the River Aire, which is downstream of Gargrave, were used to identify periods of high flow events relevant to urban flood risks. Flow events were selected using the POT method in extreme value analysis (EVA) (Leadbetter 1991). The Python package 'pyextremes' (https://georgebv.github.io/ pyextremes/) was utilised as a filtering tool for screening discrete high flow events. A functional generalisation of the generalised Pareto distribution and generalised extreme value distribution (de Fondeville and Davison 2022) was employed in the package to define threshold exceedances as 40 m³/s. Fifteen discrete flood events were initially identified, each exceeding the discharge threshold and having a time interval of more than 7 days since the preceding rainfall event. Among them, seven storm events which occurred in different months were chosen with rainfall durations of 16-60h with between 1 and >200year return periods for the coupled modelling (Table 2).

The high flow events were categorised according to event characteristics for two attributes: wet or dry antecedent conditions

 TABLE 2
 Characteristics of seven selected high flow events (the date is when the storm started).

		Event 2 (3					
	Event 1 (12 Dec 2015) (before NFM)		Event 3 (25 Dec 2015) (before NFM)	Event 4 (8 Feb 2020) (after NFM)	Event 5 (10 Oct 2019) (after NFM)	Event 6 (16 Mar 2019) (after NFM)	Event 7 (15 Feb 2020) (after NFM)
Role of each event in modelling	Calibration (baseline model)	I	Validation (baseline model)	Calibration (NFM scenarios)	Calibration (NFM scenarios)	Calibration (NFM scenarios)	Validation (NFM scenarios)
Return Period in Armley Station (~years)	50	10	> 200	100	1	20	20
Storm duration (h)	16 (single-peaked)	60 (multi- peaked)	34 (multi-peaked)	50 (single-peaked)	25 (multi-peaked)	18 (single-peaked)	23 (multi-peaked)
Total rainfall (mm)	22.4	64.0	89.6	70.2	37.0	44.6	49.2
Rainfall intensity (mm/h)	1.400	1.067	2.635	1.404	1.480	2.478	2.319
Maximum rainfall intensity (mm/h)	6.4	4.2	5.6	7.6	5.6	4.2	5.2
Simulation duration (h)	45	90.5	99	55	41.25	35	37.5
Pre-event soil conditions	Wet	Dry	Wet	Dry	Dry	Dry	Wet
Note: These date are when the event started	rted						

Note: These date are when the event started.

and single or multi-peaked. The wet and dry conditions in the catchment prior to the event were determined by the precipitation time series from Malham Tarn station and from soil moisture reports (COSMOS-UK 2020) and the Hydrological Summary for the UK (UKCEH 2012–2020). The observed flow rates from the Gargrave gauge were used to determine whether the event was single or multi-peaked.

3 | Coupling Models

3.1 | SD-TOPMODEL

SD-TOPMODEL, as a spatially distributed hydrological model (Gao et al. 2015), was used to represent and simulate land cover types and existing NFM interventions impacting soil hydrological functions and surface roughness at a catchment scale (Bond et al. 2022; Monger et al. 2024; Zhu et al. 2025). Three key parameters are employed in SD-TOPMODEL to represent these physical properties: overland flow velocity, K_v which equals 1/nwhere n is the surface roughness; soil hydraulic conductivity K_s; and soil active water storage depth m. The grid-based runoff outputs from SD-TOPMODEL at each 15-min timestep, generated by simulating land cover data and three existing NFM interventions in the catchments (woodland planting, hedgerow planting and soil aeration) (Figure 1c), were utilised as inputs for the coupled model in this study. Both parameter inputs and model outputs were grid-based and maintained a consistent resolution of 5 m, aligning with the spatially distributed framework of SD-TOPMODEL.

3.2 | Coupling Processes

After SD-TOPMODEL has completed the simulation of the entire study catchment, the sum of subsurface and surface runoff for each timestep in each 5 m grid can be obtained. The outputs include modelled runoff results from the land cover model, the combination of woodland planting, hedge planting and soil aeration (Figure 1c) and the wider catchment woodland (Figure SI.5). Most rainfall-runoff and infiltration processes occur within the sub-catchments and are predominantly driven by surface runoff after convergence to the main channel. Consequently, the flow entering the main channel is assumed to be the sum of subsurface and surface runoff from these subcatchments. This total runoff is then used as input to Flood Modeller. This process gives the opportunity to externally oneway couple SD-TOPMODEL and the hydrodynamic model at the same catchment scale. Then, the coupled model is used to simulate surface flows in the leaky dam sub-catchments and the main river channel (stream order from 7 up to 10 in the catchment) with its floodplain (Figure SI.2).

3.3 | Flood Modeller and Coupled Model

All model runs with Flood Modeller (version 7.0, Jacobs) used the alternating direction implicit (ADI) solver for 2D modelling, which computes flow depths and discharges using a method based on the 2D Saint-Venant equations (Jacobs 2022a). The ADI solver has more efficient computation of backwater effects

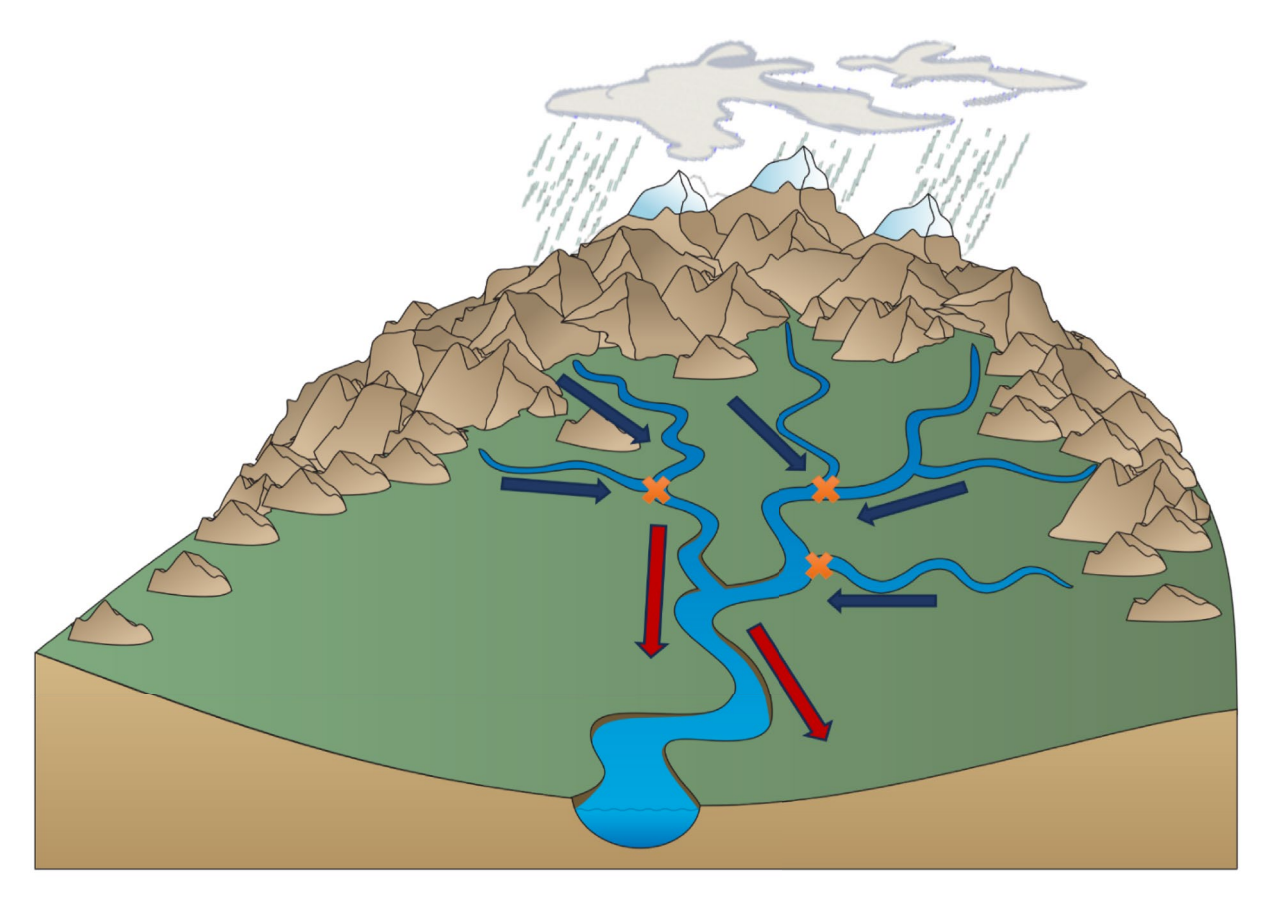
and better accuracy for mixed flow regimes, such as adding new 1D hydraulic structures (Jacobs 2022b). The coupled model was run with 1 second (s) timesteps and 5 m grid size with the same DTM elevation data as used in SD-TOPMODEL. The model parameters were set to default values except for the surface roughness parameter for the coupled model running area (Figure SI.2). The leaky dams were added into the 2D model by creating fully integrated simulations linking 2D components with embedded 1D orifice structures (Jacobs 2022c). The leaky dam sub-catchments are shown in Figure 1d. The active area for the coupled model to Gargrave, including the main channel and its floodplain, was defined using elevation data from the DTM. This area spans from the lowest elevation of the river channel to an elevation increase of 15–20 m on both sides of the channel (details of coupling method in S1).

The same SD-TOPMODEL framework as described in Zhu et al. (2025) was utilised for the coupling process. The rainfall-runoff process was conducted using the spatial distribution of soil properties and hydrological functions within SD-TOPMODEL. A sensitivity test for parameterisation for land cover and NFM interventions was undertaken for SD-TOPMODEL (Zhu et al. 2025). Spatially distributed, gridbased runoff maps (5 m grid size) for each 15-min timestep were produced. To ensure the validity of these runoff maps, a set of points was strategically selected at river junctions across the catchment. By systematically assessing the outputs from these selected grids, a representative grid for each junction was identified for subsequent point-to-point coupling procedures. The methodology for this selection process is depicted schematically in Figure 2a. In this schematic representation of the river catchment, blue arrows indicate tributary flows modelled within SD-TOPMODEL, while red arrows denote the surface flows of the main channel and its floodplain area simulated by Flood Modeller. The coupling boundaries between the two models were established at the river junctions, specifically where tributaries converge with the main channel, as denoted by the orange crosses in Figure 2a. The actual coupled model domain (covering 90.4% of the study catchment) with linked locations is illustrated in S1. At these junction points, the coupling section was executed (Figure 2b), wherein the time series runoff was extracted from the corresponding grids in the runoff maps. These time series data were subsequently used as input flow for Flood Modeller. The inflows, along with elevation data, were incorporated into the coupled model and after the addition of surface roughness changes (Table 3), the final configuration of the coupled model in Flood Modeller was completed.

3.4 | Model Calibration and Validation

3.4.1 | Calibration of Manning's *n* Roughness Coefficients

The coupled model calibration utilised the surface roughness parameter range (Manning's n roughness coefficient) as defined by Chow (1959). The calibration range for the active areas (0.035–0.060) corresponded to the classification of floodplains with 'light brush and trees in winter' as the entire area was covered by improved grassland. For the river channel, the



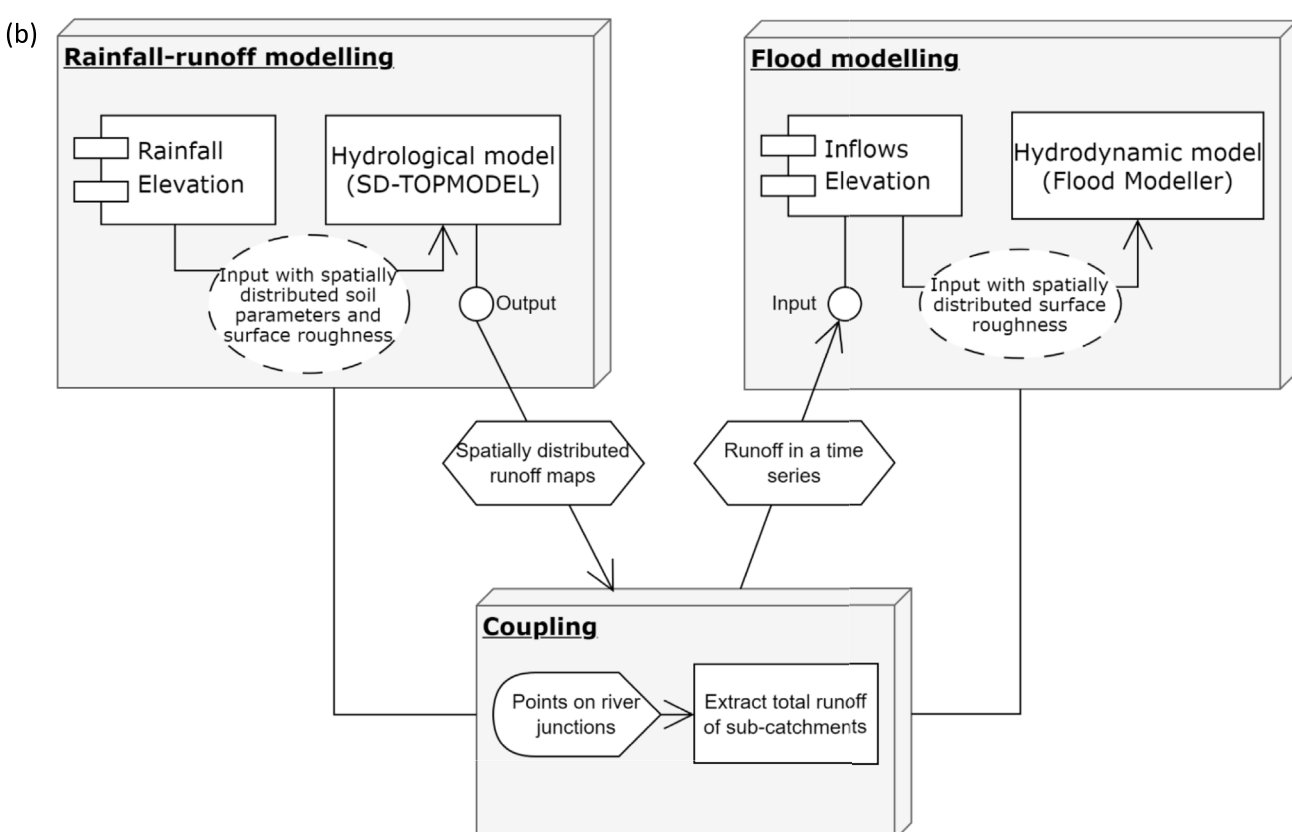


FIGURE 2 | Legend on next page.

1753318x, 2025, 4, Downloaded

from https://onlinelibrary.wiley.com/doi/10.1111/jfr3.70129 by NICE, National Institute for Health and Care Excellence, Wiley Online Library on [14/10/2025]. See the Terms

FIGURE 2 | (a) Schematic view of coupling SD-TOPMODEL to Flood Modeller 2D in the catchment (blue arrows represents hydrological flow, red arrows stand for hydrodynamic flow and the orange crosses are the schematic coupling points) and (b) coupled model structure: the smaller rectangles indicate two required inputs in each model, dashed ellipses depict model parameters and hexagons represent data used for coupling. All components are interconnected through the coupling module.

TABLE 3 | Manning's *n* roughness values used in modelling scenarios (applied in Flood Modeller 2D).

Scenario	Description	Manning's <i>n</i> roughness coefficients in the coupled model (Chow 1959)
No NFM	The catchment with land cover	0.05 (default as improved grassland) 0.03 (river channel)
NFM—leaky dams and riparian buffer strips	The catchment with land cover, a total of 228 leaky dams and riparian buffer strips applied	0.05 (default as improved grassland) 0.03 (river channel) 1.00 (area of leaky dams) 0.15 (riparian buffer strips)
NFM combination	The catchment with land cover and all NFM interventions (NFM interventions include woodland planting, hedgerow planting, soil aeration, riparian buffer strips and leaky dams)	0.05 (default as improved grassland) 0.03 (river channel) 1.00 (area of leaky dams) 0.15 (riparian buffer strips)
Wider catchment woodland	The catchment with land cover and wider catchment woodland scenario (woodland covered 66.9% area of the catchment) (Environment Agency 2024a) (Figure SI.3)	0.1 (default as sub-catchments) 0.03 (river channel) 0.15 (riparian woodland)

calibration range (0.030–0.040) reflected 'full stage, no rifts or deep pools, with stones and weeds' channel conditions, similar to the settings in Stamataki and Kjeldsen (2021). The baseline model (no NFM scenario) of the coupled model only reflects the land cover maps, which includes these two settings in Manning's n values. The baseline model was calibrated based on the 2015 Land Cover Map, then calibrated and validated with Events 1 and 3 occurring in 2015 before NFM was implemented, which may not fully reflect the actual conditions in 2012 and 2019–2020. This discrepancy may introduce some degree of uncertainty in the model's performance for these time periods. The model with NFM interventions was calibrated and validated with Events 4–7 occurring in 2019 and 2020 after NFM implementation (Table 2).

The goodness-of-fit metrics were computed from the coupled model results of the no NFM scenario and observed data across seven events and were used to evaluate model calibration within these specified ranges (S3). The final calibrated Manning's *n* values that achieve the best metrics for all seven events are shown in Table 3.

3.4.2 | Using Manning's n Roughness Coefficients to Represent NFM Interventions

Among NFM scenarios presented in Table 3, improved grassland and riparian buffer strips represented by changes in Manning's n values were incorporated into the baseline model. For the riparian buffer strips and riparian woodland, the calibration range (0.10-0.16) was applied, corresponding to the

'heavy stand of timber, a few down trees, litter undergrowth, with flood stage reaching branches' floodplain conditions. In the leaky dam sub-catchments, the predominant land cover is a mixture of grassland and woodland. For simplicity in the coupled model, a lumped roughness parameter was applied as a default value for the sub-catchments. The Manning's n roughness coefficient was set at an intermediate value of 0.10 between the calibrated values of the improved grassland (0.05) and the riparian woodland (0.15).

The friction conditions in the leaky dam implementation area can vary. Studies have shown that the Manning's *n* roughness coefficient of the leaky dam area is influenced by factors such as the density of leaky dam placement, the material and positioning of the leaky dam, streambed morphology and flow conditions (Wilcox and Wohl 2006; Shields and Alonso 2012; Turcotte et al. 2015; Addy and Wilkinson 2019). Given that the channel characteristics of the four leaky dam tributaries were very similar (Table 1) and the leaky dams were implemented by the Yorkshire Wildlife Trust according to the same material and engineered structure, factors other than flow conditions and topography were assumed to have negligible differences in these tributary catchments. During high flow events, the flow conditions at leaky dams rapidly transition from the rising limb of unsteady flow to steady overflow (Leakey et al. 2020). Resistance during water level rise was found to be two to three times higher than that after inundation, leading to afflux, adjacent floodplain connections and backwater rise during the rising phase (Shields and Alonso 2012; Keys et al. 2018; Follett et al. 2021). Consequently, Manning's n values during this process must increase significantly to account

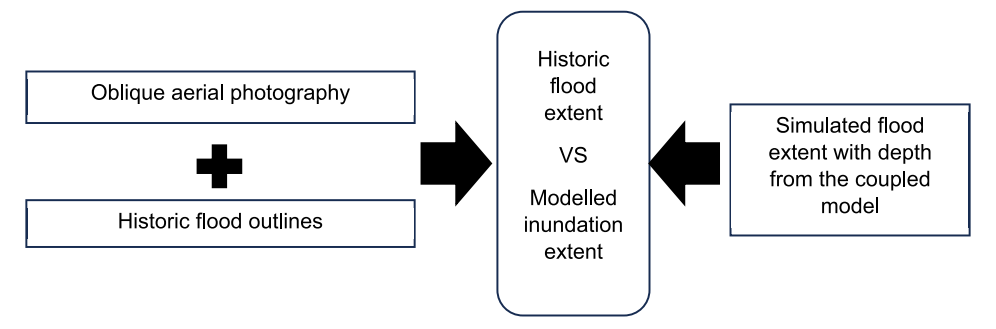


FIGURE 3 | Model validation with historic flood records.

for the added water resistance and drag forces induced by the leaky dams. The range of Manning's n values was informed by field measurements conducted by Kitts (2010) in the New Forest, England and Curran and Wohl (2003) in Washington State, USA. For similar coarse gravel bed conditions, the mean Manning's *n* values were 0.60 for step-pool and steep streams (representative of Washington streams) and 1.42 for meandering and gentle streams (New Forest, UK) under overflow. Based on these findings, the calibration range for the model was set between 0.60 and 1.50, with parameter values selected at intervals of 0.10. For simplicity, only one decimal place was retained. Ultimately, the model was calibrated to a final value of 1.0. In addition, to represent the geometric alterations to stream channels caused by leaky dams, each structure was modelled using a 1D orifice element within the hydrodynamic framework, similar to the settings in Leakey et al. (2020) and Senior et al. (2022).

3.4.3 | Model Validation

The validation of the model was conducted by comparing its output to historic flood records as well as observed hydrographs. Historic flood records were sourced from the Environment Agency's post-flood emergency oblique aerial photography (Environment Agency 2024b) and historic flood outlines (Environment Agency 2024c), which were only available for Event 3 (beginning on 25 December 2015) and Event 7 (beginning on 15 Febreuary 2020). Traces of inundation were shown in the aerial photographs and the area of inundation was determined based on geographic location and reference objects (roads, bridges and buildings). The flood inundation extents from these records were extracted and compared with the modelled inundation extents (Figure 3). The modelled inundation extents within the active area of the coupled model covered all historic records, indicating that the model performance is viable and accurate.

3.5 | Modelling Scenarios

A total of four scenarios were tested in the coupled model (Table 3). All scenarios required parameter adjustments within the coupled model to simulate these nature-based interventions. These adjustments involved modifications to both the parameters and settings in Flood Modeller. Additionally, some scenarios incorporated land cover changes and three soil and land use interventions, which required corresponding parameter

modifications in SD-TOPMODEL. These parameters in SD-TOPMODEL were calibrated and validated as described in Zhu et al. (2025), while parameterisation in Flood Modeller was described in Section 3.4 in this study.

3.5.1 | Leaky Dams and Riparian Buffer Strips Scenarios

A total of 228 leaky dams and riparian buffer strips were implemented in the catchment. This scenario was applied upon the land cover maps, requiring adjustments to Manning's n roughness coefficients in the coupled model to represent these interventions. Given that the cumulative flow mitigation effects of a large number of leaky dams were modelled at the catchment scale, minor differences between individual leaky dams were disregarded and a uniform representation was used in the coupled model, as illustrated in the schematic (Figure 4). Embedded 1D orifice structures, along with adjustments to the Manning's n roughness coefficients, were used to represent leaky dams in Flood Modeller 2D (Jacobs 2022b). As shown in the structure schematic (Figure 4), partial channel blockages were placed at each leaky dam cross section, leaving a gap (0.1–0.3 m depending on maximum elevation differences in the DTM before and after the dam) under the blockage to allow low flows to pass through. Elevation adjustments have been applied to each leaky dam to avoid overestimated back flows. With a grid size of 5 m, the model set the width of all leaky dams to 5 m and the top height of each leaky dam matched the height of the channel sides. The characteristics of the tributary catchments and the number of leaky dams are detailed in Table 1, with the average channel gradients of the four tributaries being similar, allowing for consistent height and roughness settings for all leaky dams.

3.5.2 | Land Cover, NFM Interventions and Potential Woodland Scenarios

Scenarios requiring parameter adjustments in each model include no NFM, NFM combination and wider catchment woodland scenarios (Table 3). The no NFM scenario was represented by land cover maps within the catchment, with parameters representing topsoil properties and surface roughness applied only in SD-TOPMODEL (Table 4). The calibrated surface roughness parameters for the active areas in Flood Modeller were set as default as this area was recognised as improved grassland in the land cover maps. In this case, the default Manning's *n* roughness

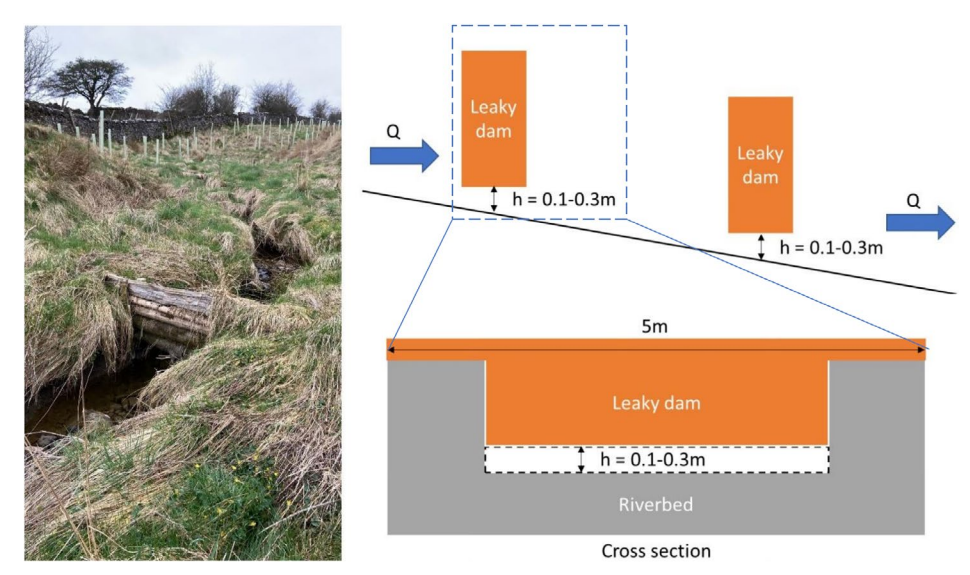


FIGURE 4 | The leaky dams and riparian buffer strips implemented in Tributary 4 (photo on 29 March 2022), schematic stream channel and cross-section of a 1D structure in the hydrodynamic model.

TABLE 4 | Calibrated parameter multiplier settings in SD-TOPMODEL for land cover types and NFM interventions.

•	•		
	Para	tipliers	
Land cover class	m (m)	k _v (–)	k _s (m/h)
Broadleaf woodland	0.0135	22.5	800
Coniferous woodland	0.0135	22.5	400
Improved grassland (baseline)	0.009	30	100
Calcareous grassland	0.009	24	300
Acid grassland	0.009	24	300
NFM interventions			
Hedgerow	0.009	15	1000
Woodland (new planted)	0.0135	18	250
Soil aeration	0.0135	30	400

Source: Zhu et al. (2025).

coefficient was used for the area and a reduced value was set as the river channel (Table 3).

The NFM combination scenario incorporated leaky dams and riparian buffer strips to the no NFM scenario, along with other NFM interventions in the catchment such as woodland planting, hedgerow planting and soil aeration modelled in SD-TOPMODEL. The setup for leaky dams and riparian buffer strips followed Table 3, while other interventions were consistent with all NFM scenarios described being used within SD-TOPMODEL in Table 4. The wider catchment woodland scenarios were based on the Catchment Woodland Potential map from Environment Agency, which used the same parameter settings as the NFM intervention woodland planting (new woodland) in SD-TOPMODEL. In Flood Modeller, the potential woodland in the active area applied the same Manning's n roughness coefficient

as riparian buffer strips. Thus, all scenarios were fully implemented in the coupled model.

4 | Results

4.1 | Coupled Model Performance for Various High Flow Events

The model performance of the calibrated coupled model was evaluated by goodness-of-fit metrics calculated between the no NFM scenario results and observed data (Table 5). The model demonstrates a good overall fit for all events except Event 2. For example, NSE, R^2 , VE and KGE were all greater than 0.6. Optimal values for each metric were achieved in Event 3, where RMSE and PBIAS were both close to 0, while other metrics approached 1. In contrast, Event 2 (occurring in 2012) showed a poor fit for some metrics (e.g., NSE of -0.02 and R^2 of -0.02), though wNSE, VE and KGE values improved (ranging between 0.4 and 0.5) due to their focus on flood peaks, even when the overall fit remains suboptimal. Events 4-7 (occurring between 2019 and 2020) also showed a lower fit compared to Events 1 and 3, which occurred in 2015. This may be attributed to the baseline model's use of the 2015 land cover map, which may differ slightly from land cover in other years. Some NFM interventions had been implemented in the catchment by 2019-2020, which are not included in the baseline model (no NFM scenario) for simulation of Events 4-7.

Model performance is also affected by the characteristics of high-flow events. When catchment preconditions are dry, the lack of an infiltration simulation module in the coupled model results in less water loss in the simulation, especially compared to wet conditions. Events 2, 5, 6 and 7 are small to medium-sized flood events with return periods from 1 to 20 years, with lower peak discharge than more extreme events (return periods from 50 to > 200 years). The receding limbs of these small peaks are more affected by infiltration processes.

TABLE 5 | Goodness-of-fit metrics for coupled model results (no NFM) with calibrated Manning's *n* values (Table 3) applied across seven events (Metrics' attributes in Table SI.1).

	Event 1	Event 2	Event 3	Event 4	Event 5	Event 6	Event 7
RMSE	6.95	8.56	4.74	9.53	7.9	9.54	9.78
PBIAS %	18.10	57.30	-0.30	-10.70	37.30	30.20	31.20
NSE	0.81	-0.02	0.95	0.83	0.61	0.68	0.67
wNSE	0.89	0.49	0.94	0.81	0.69	0.59	0.75
d	0.94	0.79	0.99	0.95	0.92	0.94	0.92
r	0.94	0.9	0.98	0.94	0.96	0.99	0.97
R^2	0.81	-0.02	0.95	0.83	0.61	0.68	0.67
VE	0.69	0.41	0.91	0.81	0.62	0.70	0.69
KGE	0.71	0.42	0.97	0.74	0.6	0.65	0.68

This effect is more pronounced in Event 2, which has lower flow and multiple flood peaks. While the discharge and timing of flood peaks are well-matched in the hydrographs of model results, the peak recession process diverges from observed data. This discrepancy is also evident in goodness-of-fit metrics but does not compromise the accuracy of the model in simulating peak times and other high flow peaks. Therefore, the characteristics of the coupled model allow it to accomplish a good fit for extreme flood events with return periods greater than 50 years and to ensure the modelling accuracy of flood peak discharge and timing for small to medium flood events (1–20 years of return period).

4.2 | Flood Mitigation Impacts of NFM Scenarios

4.2.1 | Impacts of Leaky Dams on Tributaries

Because the four sub-catchments are all upland, they share similar soil and landscape characteristics, though other characteristics differ, as shown in Table 1. However, integrating the simulation results for the seven events revealed notable differences among the tributaries. The effects on peak delay and peak discharge reduction were inversely proportional among the four tributaries; in one tributary, a higher delay time was often coupled with a smaller peak discharge reduction (Figure 5). For example, in Tributary 2, results showed effective peak delays ranging from 30 to 75 min across seven events, alongside increased peak discharge for all but one event. Similar inverse effects appeared in the other three tributaries, although not as markedly as in Tributary 2. In contrast, differences between events within the same tributary were minimal, shown as outliers in Figure 5 with only five outliers present overall. In general, leaky dams resulted in peak delays in all four tributaries, with mean values ranging from 8.6 to 60 min; except for Tributary 1, which had a greater reduction in peak discharge (mean 1.84%) and the other three tributaries, which had subtle reductions (mean values ranging from 0.53% to 0.63%). Therefore, the peak delay effect of leaky dams is greater than the effect on flood peak reduction.

4.2.2 \mid Catchment-Scale NFM Scenario Impacts on Flood Peaks

The flood mitigation effects across three NFM scenarios were evaluated by comparing the percentage of peak discharge reduction and the time lag between flood peaks relative to the no NFM scenario (Figure 6). All scenarios demonstrated positive flood mitigation impacts, yet differences were observed across various high-flow events and NFM scenarios.

Among the events, Event 1 exhibited the highest peak reduction percentages across all scenarios, while Events 2 and 5 showed small flood reductions (> 1%) and Events 3, 4, 6 7 experienced only minimal peak reductions (< 0.5%). Notably, peak delay impacts did not always correspond to peak reductions in certain events. For example, Events 4 and 6 displayed flood delays of up to 15 min despite minimal peak reductions, while Events 1 and 5 achieved greater peak reductions with comparable or smaller peak delays in NFM (leaky dams and riparian buffer strips) and NFM combination scenarios. These variations in flood peak behaviour are also depicted in the hydrographs (Figure 7). These differences between events are likely influenced by specific event characteristics. For instance, two of the seven high flow events, extreme Events 3 (with a return period exceeding 200 years) and 4 (with a return period of 100 years) both showed flood reduction effects of less than a 0.5%. However, this pattern did not hold for Events 6 and 7, both with 20-year return periods, which experienced high average rainfall intensities that may have diminished flood mitigation effects in the modelling results. This feature was similarly reflected in the peak delay results: Events 3, 5 and 7 showed no delays for NFM (leaky dams and riparian buffer strips) and NFM combination scenarios.

While the pattern of differences between events remained consistent across scenarios, there were subtle variations in event responses between scenarios. The hydrographs indicated that the runoff results for the NFM (leaky dams and riparian buffer strips) scenario and NFM combination scenario were very similar, with only minor non-overlapping peaks. This was

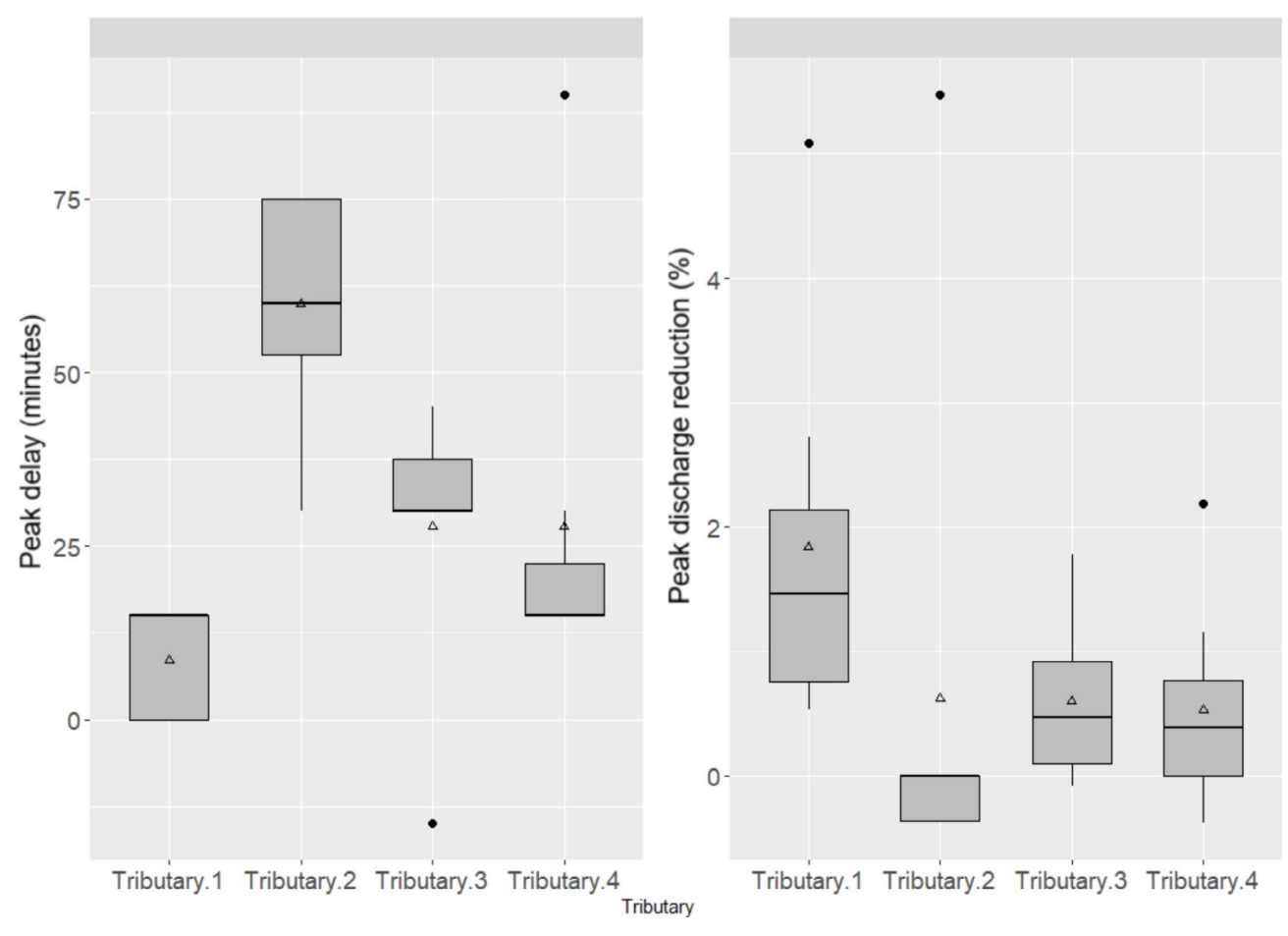


FIGURE 5 | Impacts of leaky dam implementation on peak delay (minutes) and peak discharge reduction (%) in seven events grouped by four leaky dam tributaries (the triangle represents the mean value; the line is the median value).

consistent, as shown in Figure 6, where the percentage of peak reduction increased in the NFM combination scenario except for Events 1 and 2, with only Event 2 showing an increase in peak delay time.

In contrast, the wider catchment woodland scenario caused more marked changes across all seven events, as shown in Figure 6 and in the hydrographs in Figure 7. Peak reduction percentages and delay times increased compared to the other two scenarios, especially in Events 4, 6 and 7, which had only minor reductions in the other two scenarios. Increases were smaller for extreme Events 3, with only a minimal rise (from 0.03% to 0.14%). The impact of the wider catchment woodland scenario on peak delays was also significant: all events showed notable increases in peak delay time of 30-60 min. This effect is clearly visible in the hydrographs for each event, where all rising limbs are flattened and slowed, resulting in delays for both single and multiple flood peaks. The increases in delay times did not vary greatly across events, suggesting minimal influence from event characteristics, except flood magnitude (return period). Overall, the NFM combination scenarios offer slightly improved flood mitigation than the NFM (leaky dams and riparian buffer strips) scenario, while the wider catchment woodland scenario significantly enhanced flood mitigation compared to the other two scenarios. This indicates adding more intervention types in the catchment is not beneficial for all events.

4.2.3 | Impacts on Flood Inundation Extent and Depths

In addition to evaluating peak discharge reduction and peak delay times, the coupled model also produced inundation extent and depth results for each high flow event. Taking Event 1 as an example, Figure 8 illustrates the maximum extent and depth of inundation near the downstream end of the study catchment (around Gargrave town) for this event under different NFM scenarios, which varied noticeably between scenarios.

Firstly, there are variations in the flood inundation extent. The NFM (leaky dams and riparian buffer strips) scenario exhibited the smallest inundation area under the same rainfall conditions, closely followed by the NFM combination scenario. Compared to the no NFM scenario, these two scenarios resulted in reduced inundation at critical points, such as on roads on the edge of the reach (notably Skipton Road and High Street in Gargrave town centre) and overflow around the railway and Priest Holme Bridge, both of which are highlighted in Figure 8a. These reductions in inundation extent are significant improvements. However, the wider catchment woodland scenario increased the maximum extent of inundation by 4.4% of the coupled model area, which was reflected across all the demonstration areas in Figure 8. This expansion of the inundation was, particularly, pronounced in Gargrave town, including roads, green spaces and some residential areas. This outcome

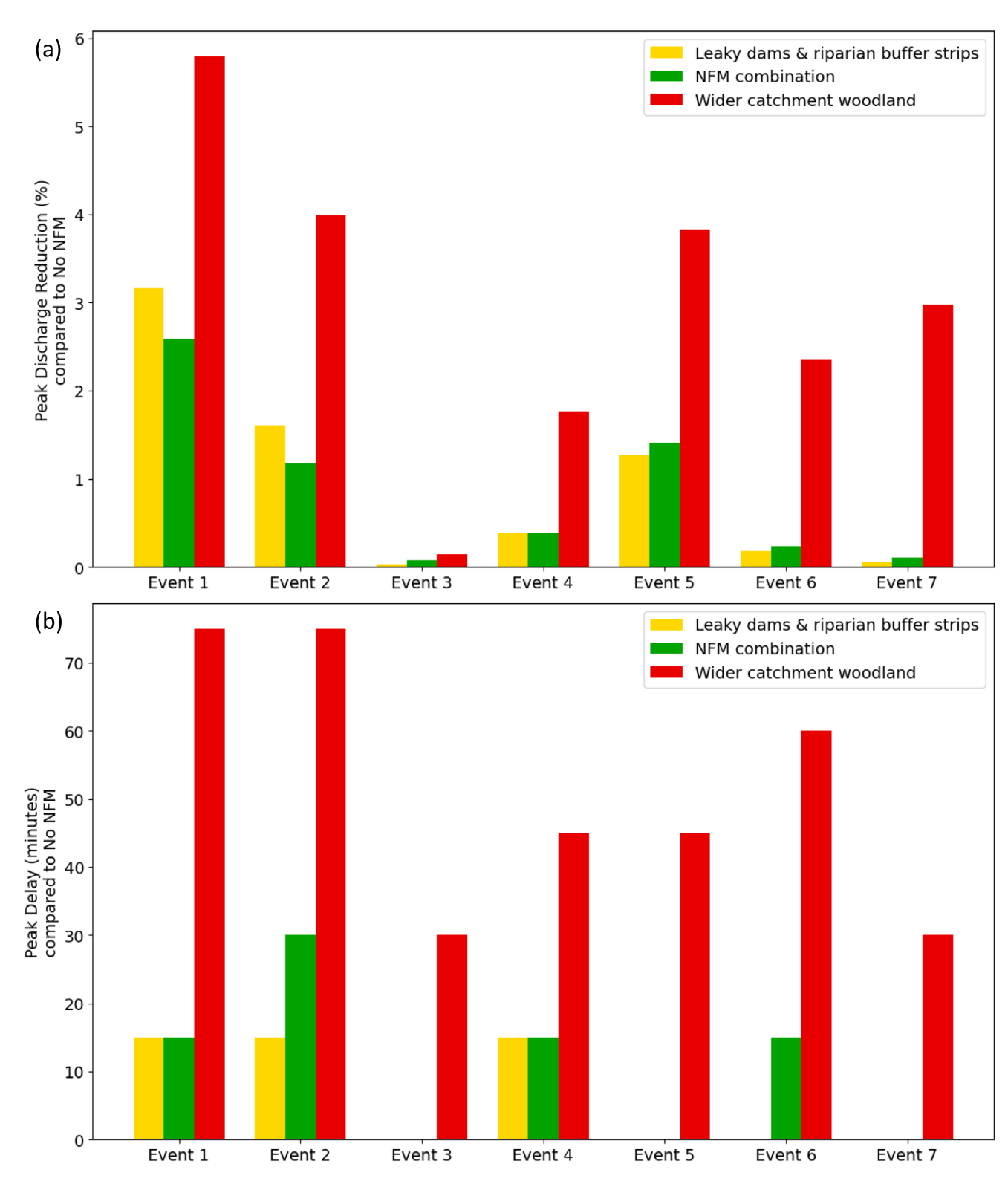


FIGURE 6 | Flood mitigation results from the coupled model by comparing NFM scenarios with the no NFM scenario. (a) Peak discharge reduction and (b) peak delay.

contradicts the findings that the wider catchment woodland scenario achieved greater peak discharge reduction and peak delay. The apparent contradiction arises because extensive tree planting in this scenario increases surface roughness in the catchment, thus slowing down the flow. These changes in runoff may cause peak flow synchronisation. Also, the prolonged

runoff process on the floodplain led to a higher number of wet cells in the coupled model area compared to the other three scenarios, as indicated by the model results. This suggests greater overland flow within the catchment, including overflow onto floodplains and channel perimeter, resulting in a larger inundation extent.

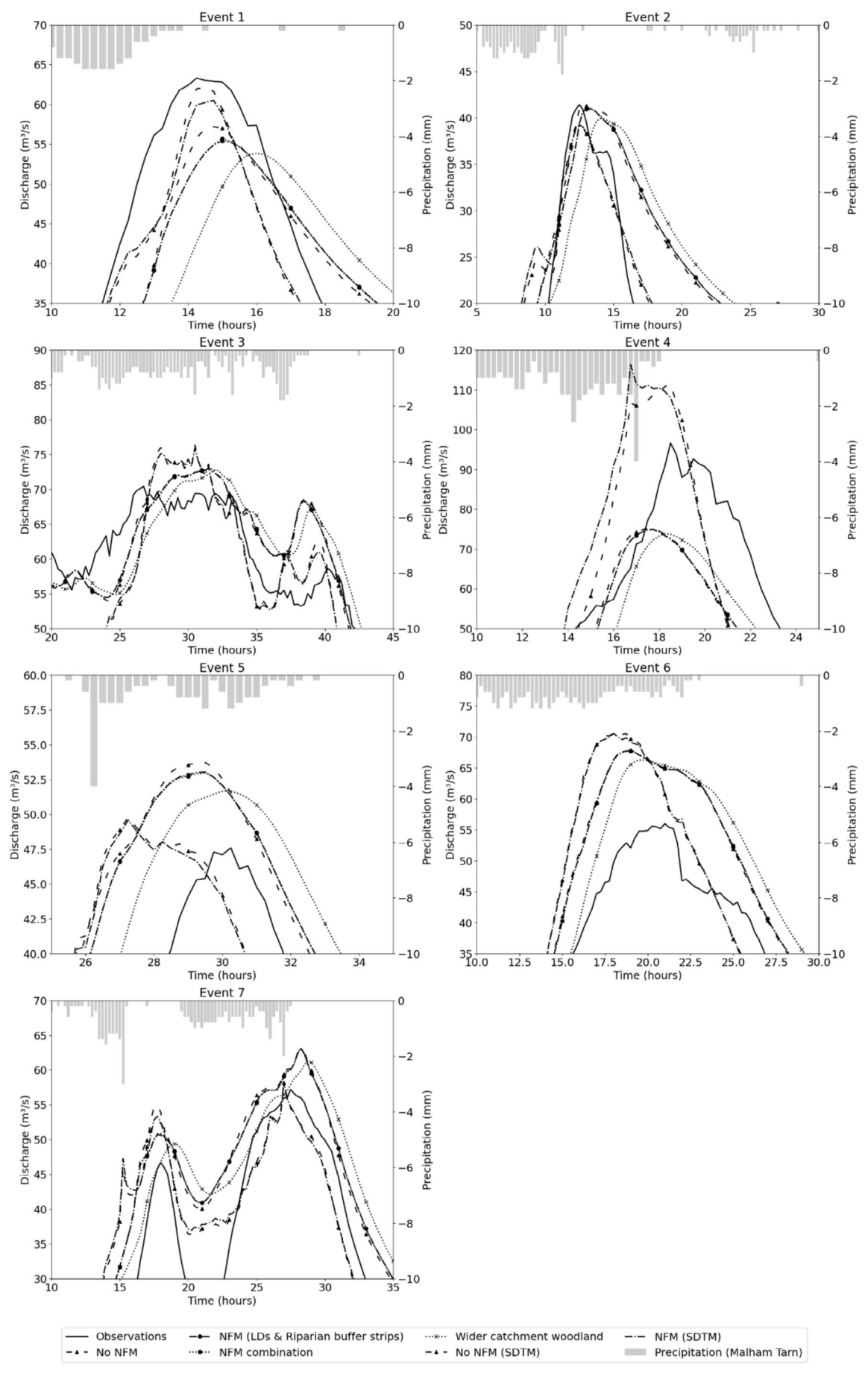


FIGURE 7 | Legend on next page.

FIGURE 7 | Hydrographs of peaks for seven events produced by the coupled model (no NFM, NFM—leaky dams and riparian buffer strips, NFM combination, wider catchment woodland scenarios) and SD-TOPMODEL (no NFM and NFM scenarios). Full hydrographs are in S2.



FIGURE 8 | Coupled model outputs of maximum inundation extents and depths (m) among different scenarios (Event 1) for the large village of Gargrave. (a) No NFM scenario; (b) Leaky dams and riparian buffer strips scenario; (c) NFM combination scenario; (d) Wider catchment woodland scenario.

When comparing the maximum inundation depths, the results for the two NFM implementation scenarios and the no NFM scenario are generally similar, with differences of less than 0.5 m in most areas. This aligns with previous findings for peak discharge, where reductions due to NFM interventions were not substantial. However, in the wider catchment woodland scenario, significant increases in maximum inundation depth were observed across inundated areas. Distinct colour changes in Figure 8 highlight regions where inundation depth increased. This suggests that the NFM (leaky dams and riparian buffer strips) scenario and the NFM combination scenario effectively reduce critical inundation extents, but their impact on inundation depth is minimal. Conversely, the wider catchment woodland scenario may exacerbate potential flood risk due to increases in both maximum inundation extent and depth.

4.3 | Assessing Model Performance of the Coupled Model in Comparison to SD-TOPMODEL

The hydrographs also included the results of the SD-TOPMODEL simulations (only the scenarios with land cover and all NFM interventions were shown as no NFM and with NFM in Figure 7) to compare the performance of the coupled model with SD-TOPMODEL. The hydrographs indicated that SD-TOPMODEL generally provided a better fit between simulated runoff and observed data for most events (e.g., Events 1, 2, 3, 5 and 7), while overestimation of peak discharge occurred in Events 4 and 6. Notably, these overestimations were mitigated in the coupled model results. This pattern was consistent across all events but did not always result in a decrease; in some cases, the coupled model showed increased peak discharge. A distinguishing feature of the coupled model compared to SD-TOPMODEL was

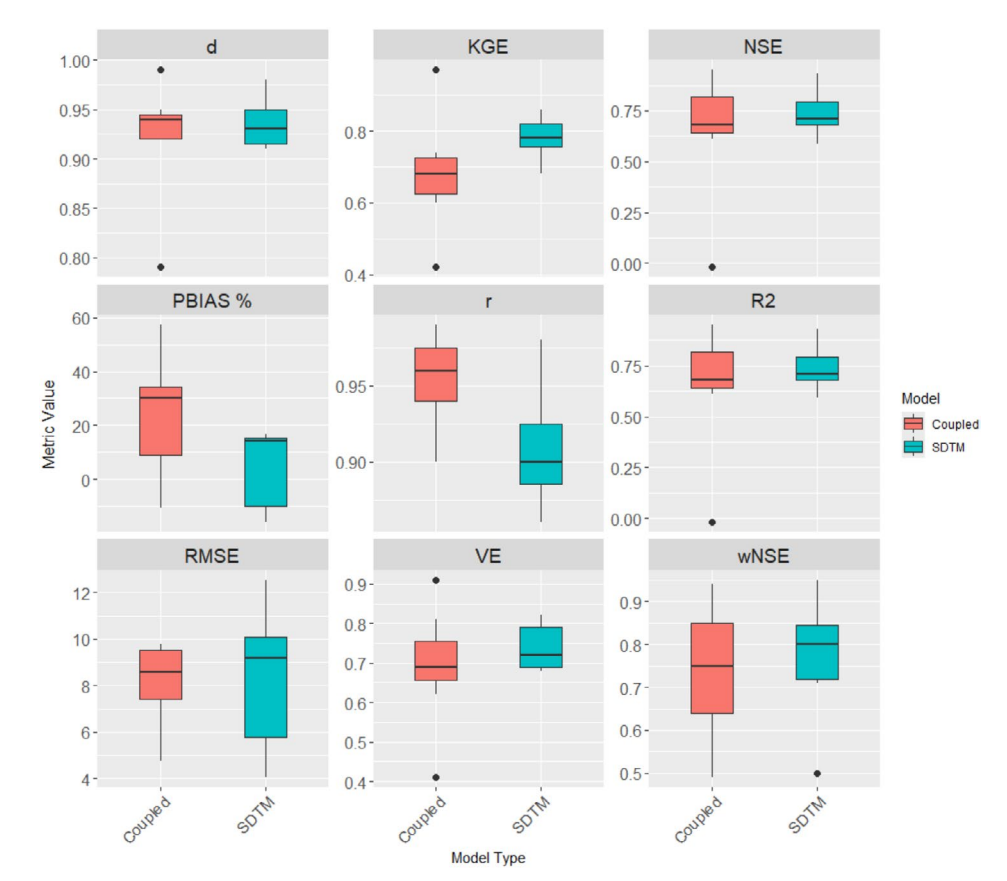


FIGURE 9 | Comparison of goodness-of-fit metrics calculated for seven events (no NFM scenario) between SD-TOPMODEL (SD-TM) and the coupled model.

its ability to flatten flood peaks and reduce hydrograph fluctuations. For multi-peaked events, the second or subsequent peaks were often elevated. This behaviour is likely due to the coupled model's lack of an infiltration module in its computing mechanism. Focusing on the localisation of the flood peaks, the coupled model provided a better fit for peak shapes and discharge compared to SD-TOPMODEL. This was especially evident in the arrival time of peaks, where the coupled model results showed strong consistency with observed data.

In addition to the visual inspection of the hydrographs, goodness-of-fit metrics were employed as statistical criteria to assess the baseline models of both the coupled model and SD-TOPMODEL for model accuracy. The box plot (Figure 9) illustrates the comparison between the coupled model and SD-TOPMODEL across nine goodness-of-fit metrics (S3), calculated from seven events under the no NFM scenario (land cover map applied only) and the observed data.

First, the model performance indices (d, KGE, r, VE, NSE, R^2 , wNSE) are compared: the results for d, NSE, R^2 and wNSE are similar between the two models, with the coupled model having slightly better NSE and R^2 values than SD-TOPMODEL. For the Pearson correlation coefficient (r), the coupled model shows better performance. Conversely, SD-TOPMODEL slightly outperforms the coupled model in KGE and VE, though outliers representing over- and under-performance are observed in the coupled model results. Metrics such as NSE, R^2 and d are lumped criteria, insensitive to the variability in

the results, while KGE and VE are normalised by the average observation, leading to an underestimation of peak discharge (Althoff and Rodrigues 2021). The wNSE metric increases the weighting of the peak discharge to address the limitation of NSE (Hundecha and Bárdossy 2004). Pearson's r reflected the correlation between the modelled results and observed data, indicating that the trends are closely aligned. For error measures, the coupled model provides worse results than SD-TOPMODEL in PBIAS, a metric normalised by the average of observed values. However, as RMSE assigns greater weight to larger errors and outliers, the coupled model achieves a lower RMSE value, indicating smaller absolute errors compared to SD-TOPMODEL.

Overall, these assessment metrics demonstrate that the coupled model and SD-TOPMODEL exhibit comparable accuracy, with the coupled model outperforming SD-TOPMODEL in capturing flood peaks and peak rates. The coupled model does not simulate the receding limb as effectively as SD-TOPMODEL, which is reflected in several metrics normalised by means. The coupled model provides better performance in metrics emphasising peaks and outliers.

4.4 | Variations Between the Coupled Model and SD-TOPMODEL in Responses to NFM

The differences in discharge over time generated by the two models simulating the catchment with or without NFM

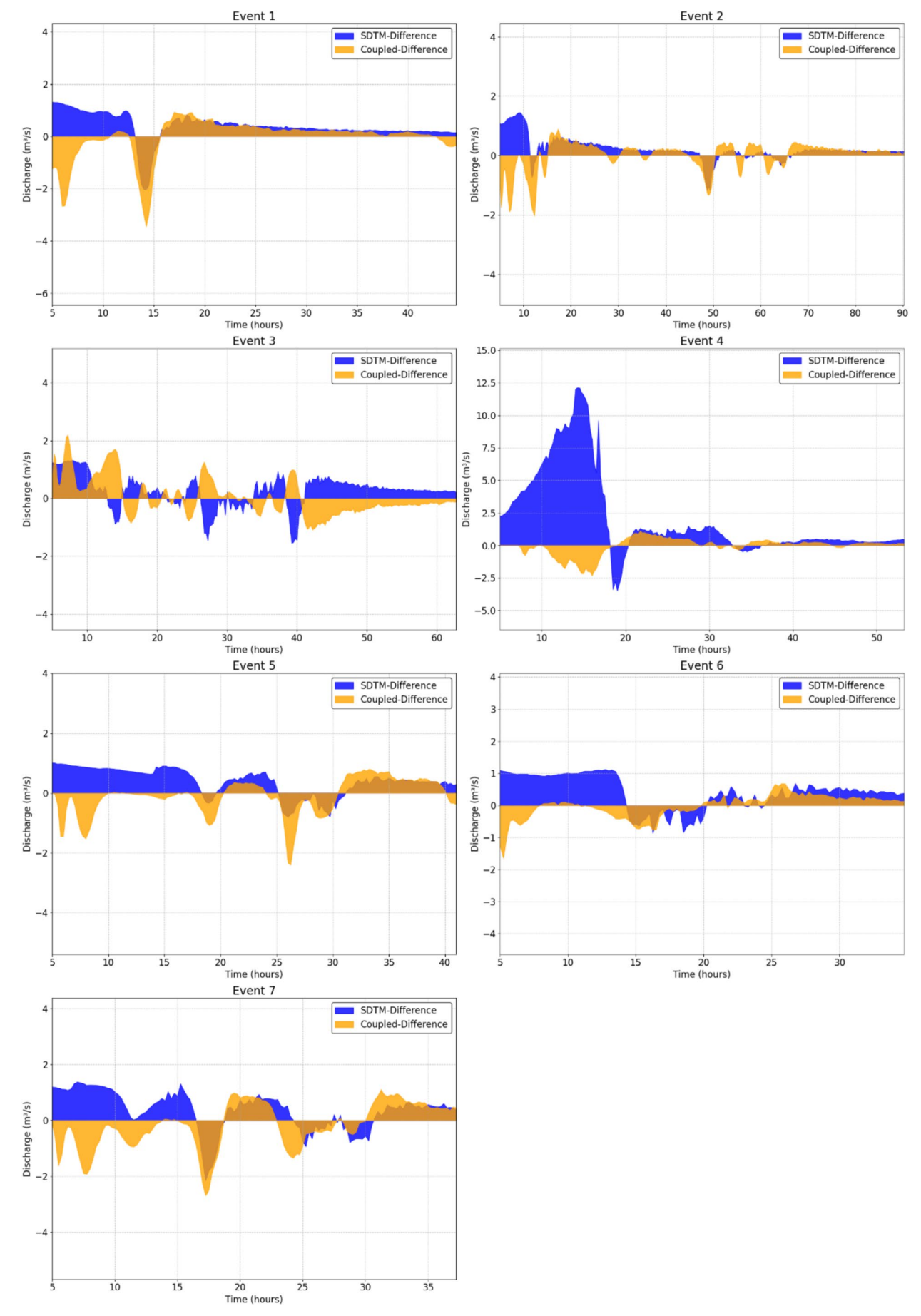


FIGURE 10 | Legend on next page.

FIGURE 10 | The discharge differences between no NFM and with NFM in SD-TOPMODEL (SDTM) and the coupled model (positive values represent increases in discharge by using NFM discharge minus no NFM discharge and vice versa). Full details of the event hydrographs are shown in Figure SI.4.

interventions for each of the seven events are illustrated in Figure 10. These comparisons highlight how the coupled model maintains robustness in simulating NFM effectiveness while exhibiting distinct model characteristics. Additionally, they illustrate the models' performance under different highflow event characteristics. A consistent feature across all events was that the SD-TOPMODEL simulation under NFM scenarios increased total runoff during the period of the rising limb following rainfall onset compared with the no NFM scenario, whereas the coupled model generally showed a decrease. This difference arises because SD-TOPMODEL represents NFM interventions as increasing soil infiltration and water storage, resulting in a rapid increase in subsurface runoff after rainfall onset along with a rapid increase in total runoff in the final output of the model. This is a process that is not fully delivered in the coupled model. In contrast, the Flood Modeller part accounts for NFM interventions by increasing surface roughness, which could reduce runoff after rainfall onset. An exception occurred in Event 3, where intense and concentrated rainfall rendered increased surface roughness insufficient to reduce runoff effectively.

During the flood peak period, the timing and discharge of peak differences were broadly consistent between the two models, with similar reductions observed. However, some deviations were evident in specific events, likely influenced by event characteristics. For example, in Events 3 and 4, which were characterised by high-intensity continuous rainfall, the models exhibited asynchronous responses to NFM interventions. In the hydrograph for Event 3 (Figure 7), prolonged high flow resulted in unsynchronised hydrograph shapes and NFM-induced variations between the models, driven by reduced fluctuations in the coupled model. Event 4, occurring under dry antecedent catchment conditions, revealed SD-TOPMODEL's heightened sensitivity to high-intensity rainfall with the addition of NFM, producing substantial increases in total runoff. Conversely, the coupled model reduced runoff due to increased surface roughness. In other high-flow events, the NFM simulations by the two models were unaffected by multi-peaked floods or varying catchment conditions (wet or dry).

Thus, the coupled model demonstrated some divergence from SD-TOPMODEL under high-intensity rainfall events but retained robustness and reliability in simulating NFM scenarios. It also provided robust insights into the impacts of NFM interventions on peak discharge and timing, affirming its suitability for NFM intervention modelling.

5 | Discussion

Using the coupled model, all NFM interventions in the study catchment were integrated into the catchment-scale modelling framework, including detailed representations of leaky dams and other surface structural measures. This approach provides opportunities to evaluate the effectiveness of NFM interventions and assess their potential impacts on tributary synchronisation under various rainfall events and NFM scenarios at larger catchment scales.

5.1 | The Effectiveness of Leaky Dams by Scale

In this study, experimental comparisons were conducted using the coupled model to evaluate the effects of leaky dams in four tributaries before and after their implementation. Previous studies suggested that leaky dams were most effective for events with a return period less than 1.5 years, with diminishing peak reduction effectiveness as the return period increases (Senior et al. 2022; van Leeuwen et al. 2024). However, no reduction in effectiveness with increasing return periods of events (from 1 to > 200 years) was observed in this study. While no significant differences in effectiveness were found across event characteristics, results varied between tributaries. These variations showed no correlation with tributary catchment area or the number of leaky dam implementations, supporting findings from other modelling studies (Hankin et al. 2020; Black et al. 2021). Some studies suggested that these variations can be attributed to differences in dam physical properties, location and spacing distances and differences in geology and surface cover (Black et al. 2021; Follett and Hankin 2022). However, these factors were treated as uniform in this modelling study. Thus, the differences were most likely influenced by varying average channel gradients among the tributaries, as identical leaky dams in steeper channel gradients generate greater upstream depth and backwater volume but lower backwater length, resulting in reduced effectiveness in delaying and reducing flood peaks (Hankin et al. 2020; Follett and Hankin 2022; Follett et al. 2024).

Leaky dams were more effective at delaying flood peaks than reducing peak discharge, though these two effects were not synchronised and inversely influenced each other. A previous monitoring study observed that lag time increased with rising flood magnitudes until reaching bankfull discharge, beyond which the lag time either plateaued or decreased (Black et al. 2021). Although leaky dams facilitate the availability of floodplain connectivity and expandable field storage during high flow events, the small storage capacity of these features may impede their downstream flood mitigation impacts at the (sub-) catchment scale (Thomas and Nisbet 2012; Kay et al. 2019; Hankin et al. 2020; Beven et al. 2022; van Leeuwen et al. 2024). The findings of this study also support this, showing that both peak delay and peak reduction were less effective at the catchment scale compared to the tributary scale. All evidence points to the limited ability of leaky dams to delay and reduce flood peaks beyond the sub-catchment scale in which they are installed, but there is a lack of research on the flood mitigation potential of overflows on both sides of the overtopped dam. Further modelling is required to explore the potential for utilising expandable field storage within tributaries to better understand the relationship between peak delay and peak reduction caused by leaky dams.

5.2 | NFM Impacts on Peak Discharge and Flood Inundation

Most NFM modelling studies have concentrated on the impacts on peak discharge and timing within the flood hydrograph, with only limited attention given to the extent and depth of flood inundation (Lane 2017; Addy and Wilkinson 2019; Kay et al. 2019; Zhu et al. 2024). The coupled model utilised in this study offers detailed spatial-scale information, complementing hydrograph analyses and thus provides insightful scientific evidence for understanding the inundation impacts of NFM during high-flow events.

Some differences were observed between the outputs of SD-TOPMODEL and the coupled model. These differences were not evident when comparing the peak mitigation effects of NFM interventions, as both models achieved similar reductions in peak discharge and peak delays. However, discrepancies became apparent in the hydrographs (Figure 10), suggesting that the coupled model may have introduced additional uncertainty due to the increased complexity of the coupling process. Despite this, the coupled model offers valuable outputs of flood inundation depths and extents, which the hydrological model alone cannot provide. This distinction informs the targeted use of each model in NFM modelling. In upland catchments, where rainfall-runoff processes dominate, SD-TOPMODEL offers a more efficient modelling approach. Conversely, in scenarios involving surface structures, runoff convergence and floodplain inundation, the coupled model is more appropriate due to its ability to simulate flood inundation dynamics.

This study reveals that under NFM scenarios, both inundation extent and depth decrease as peak discharge decreases. However, large-scale tree planting across the catchment, despite reducing peak discharge, increases inundation extent and depth. The effects of increased woodland on flood peaks remain debated, with evidence suggesting reduced effectiveness for larger flood events and in larger catchments (Xiao et al. 2022). This observation aligns with the results in Figure 6, where the reduction in flood peaks is smaller for extreme events such as Events 3 and 4, which have return periods \geq 100 years. Additionally, previous studies have concluded that woodland effectiveness is highly related to its desynchronisation of flood waves through the catchment (Dixon et al. 2016; Dadson et al. 2017; Lane 2017; Metcalfe et al. 2018; Kingsbury-Smith et al. 2023).

The coupled model accounts for two critical effects caused by woodland: slowing the process of saturation-excess overland flow (Murphy et al. 2020) and increasing surface roughness during the conveyance of overland flow across the catchment (Bond et al. 2020; Monger et al. 2022, 2024). A plausible explanation for the model results is that these effects may inadvertently synchronise flood wave arrivals downstream under the ideal maximum woodland scenario. While upstream woodland reduces total runoff (as seen in hydrograph runoff reductions), delayed streamflow and overland flow may arrive simultaneously

downstream, leading to a greater inundation extent and depth, particularly, in Gargrave town. This finding underscores the need to understand interactions between NFM interventions, as poorly coordinated designs within sub-catchments could result in unintended synchronisations (Blanc et al. 2012; Pattison et al. 2014; Dixon et al. 2016). Thus, it is strongly recommended that modelling is undertaken for all catchments where NFM interventions are proposed to ensure effective planning mitigates such synchronicity risks and optimises spatial designs.

5.3 | Benefits and Future Implications of the Coupled Model

Even though SD-TOPMODEL has enabled spatially distributed simulations at high resolutions (Gao et al. 2015, 2017; Kingsbury-Smith et al. 2023), its outputs remain constrained by the TOPMODEL algorithm, which produces spatial-scaled, cumulative and conceptual results. These outputs are primarily valid at river channels and their confluences and catchment outflow boundaries, in alignment with hydrological principles. However, the model's outputs in accumulation areas, such as hillslopes, are stochastic and do not provide detailed hydrological insights. The coupling of SD-TOPMODEL and Flood Modeller 2D enhances their capabilities by enabling the input of precise surface structural changes, such as leaky dams, into the model and by producing fully spatially distributed outputs.

The direct coupling of a hydrological and 2D hydrodynamic model at the same scale, as implemented in this study, is computationally more efficient than using a 2D hydrodynamic model alone to simulate surface runoff across the whole region (Shen et al. 2024). In the rainfall process, runoff flows through both the hydrological model and the 2D hydrodynamic model regions simultaneously. Using this direct coupling method synchronises the rainfall-runoff and surface convergence processes, allowing the model to represent flooding dynamics more accurately (Brewer et al. 2018). Furthermore, goodness-of-fit metrics used to evaluate model performance demonstrate that the coupled model achieves high accuracy and performs, particularly, well in simulating flood events with high return periods. This improved performance can be attributed to the computational mechanisms and default parameters inherent in Flood Modeller 2D (Pinos and Timbe 2019). Thus, the coupled model effectively incorporates SD-TOPMODEL's operational mechanisms for soil property changes and rainfall-runoff processes, maintaining both accuracy and performance while providing enhanced spatiotemporal outputs.

However, the coupled model faced certain limitations. One significant limitation was the representation of leaky dams, which was constrained by the model's 5 m resolution. This constraint required all leaky dams to be represented with a uniform width of 5 m, potentially overestimating or underestimating their real-world physical characteristics. Additionally, a common challenge in NFM modelling is the limited availability of post-implementation monitoring data for model validation (Hill et al. 2023). In this study, the inundation validation of the coupled model, which relied on historical flood records, demonstrated limited accuracy, thereby introducing potential uncertainties

into the model outputs. Thus, more empirical data from field measurements are needed to validate the model results.

The coupling method employed in this study was developed specifically for SD-TOPMODEL and requires further validation for its application across other hydrological and hydrodynamic models. Currently, the approach involves manually identifying coupling points and extracting runoff data, which limits its scalability and efficiency. Future advancements could focus on developing automated processes through coding, incorporating necessary parameters to streamline the coupling workflow. Additionally, the next stage of research should aim to model systematic NFM interventions at a catchment scale, enabling simulations at larger scales (100–1000km²) and across diverse catchments with varying characteristics. Such advancements will provide robust, numerical evidence to support NFM planning and inform future policy development.

6 | Conclusions

This study used a coupled hydrological-hydrodynamic model to evaluate the effectiveness of multiple NFM interventions. including woodland planting, hedge planting, soil aeration, riparian buffer strips and leaky dams and their influence on flood peak delay, discharge reduction and inundation extents and depths for high flow events in a large-scale catchment (81.4km²). The coupling approach between SD-TOPMODEL and Flood Modeller 2D demonstrated a good fit and reliable performance for both peak discharge and timing simulations. The study also revealed that leaky dams are more effective in delaying flood peaks than in reducing peak discharge in the tributary catchments and their impacts at the larger catchment scale are similar to that provided by the combination of all NFM interventions. While NFM scenarios consistently showed positive flood mitigation impacts with reductions in peak discharge, inundation extent and depth, the maximum woodland scenario across the catchment unexpectedly increased inundation extent and depth due to the potential synchronisation of flood wave arrivals downstream and increased surface roughness on floodplains. These results highlight the critical need for coordinated NFM planning to avoid unintended synchronisation and optimise intervention effectiveness. While practitioners may be keen to simply go ahead and apply NFM and land cover interventions based on anticipated 'typical' flood outcomes, catchment-by-catchment modelling is necessary to reduce the possibility of inadvertent impacts being realised. Such modelling has a cost implication for catchment planners, but ultimately this consists of a very small component of the overall cost of implementing an NFM scheme at scale and is trivial compared to the scale of costs associated with flood damage to properties and infrastructure. Overall, the coupling of SD-TOPMODEL with Flood Modeller 2D proved robust, offering enhanced spatiotemporal inundation outputs and a valuable tool for modelling the impacts of NFM interventions on flood hazards in downstream towns and cities. It also enabled the precise incorporation of structural changes such as leaky dams and spatial changes such as land and soil management at a catchment scale larger than 50 km², demonstrating its utility for integrated catchment-scale NFM modelling.

Acknowledgements

This work was undertaken on ARC3/ARC4, part of the High-Performance Computing facilities at the University of Leeds, UK. NFM records and data in Upper Aire Catchment were provided by Yorkshire Wildlife Trust. We thank two anonymous reviewers and the editors for providing constructive feedback that improved this manuscript.

Conflicts of Interest

The authors declare no direct conflicts of interest. J.H. is currently funded to undertake flood and nature-based solutions research by West Yorkshire Combined Authority, Leeds City Council, Research England, European Commission and Innovate UK. M.K. is currently funded to undertake nature-based solutions policy research by Research England.

Data Availability Statement

The data that supports the findings of this study are available in the Supporting Information of this article.

References

Addy, S., and M. E. Wilkinson. 2019. "Representing Natural and Artificial In-Channel Large Wood in Numerical Hydraulic and Hydrological Models." *WIREs Water* 6, no. 6: e1389.

Alaoui, A., M. Rogger, S. Peth, and G. Blöschl. 2018. "Does Soil Compaction Increase Floods? A Review." *Journal of Hydrology* 557: 631–642.

Althoff, D., and L. N. Rodrigues. 2021. "Goodness-Of-Fit Criteria for Hydrological Models: Model Calibration and Performance Assessment." *Journal of Hydrology* 600: 126674.

Archer, N. A. L., M. Bonell, N. Coles, A. M. MacDonald, C. A. Auton, and R. Stevenson. 2013. "Soil Characteristics and Landcover Relationships on Soil Hydraulic Conductivity at a Hillslope Scale: A View Towards Local Flood Management." *Journal of Hydrology* 497: 208–222.

Bark, R. H., J. Martin-Ortega, and K. A. Waylen. 2021. "Stakeholders' Views on Natural Flood Management: Implications for the Nature-Based Solutions Paradigm Shift?" *Environmental Science & Policy* 115: 91–98.

Barnes, M. S., J. C. Bathurst, E. Lewis, and P. F. Quinn. 2023. "Leaky Dams Augment Afforestation to Mitigate Catchment Scale Flooding." *Hydrological Processes* 37, no. 6: e14920.

Barnsley, I., R. Spake, J. Sheffield, J. Leyland, T. Sykes, and D. Sear. 2021. "Exploring the Capability of Natural Flood Management Approaches in Groundwater-Dominated Chalk Streams." *Water* 13, no. 16: 2212.

Beven, K., T. Page, B. Hankin, et al. 2022. "Deciding on Fitness-For-Purpose-Of Models and of Natural Flood Management." *Hydrological Processes* 36, no. 11: e14752.

Black, A., L. Peskett, A. MacDonald, et al. 2021. "Natural Flood Management, Lag Time and Catchment Scale: Results From an Empirical Nested Catchment Study." *Journal of Flood Risk Management* 14, no. 3: e12717.

Blanc, J., G. B. Wright, and S. Arthur. 2012. NFM Knowledge System, Part 2—The Effect of NFM Features on the Desynchronising of Flood Peaks at a Catchment Scale. CREW. http://www.crew.ac.uk/projects/natural-flood-management.

Bond, S., M. J. Kirkby, J. Johnston, A. Crowle, and J. Holden. 2020. "Seasonal Vegetation and Management Influence Overland Flow Velocity and Roughness in Upland Grasslands." *Hydrological Processes* 34, no. 18: 3777–3791.

Bond, S., T. Willis, J. Johnston, et al. 2022. "The Influence of Land Management and Seasonal Changes in Surface Vegetation on Flood Mitigation in Two UK Upland Catchments." *Hydrological Processes* 36, no. 12: e14766.

Brewer, S. K., T. A. Worthington, R. Mollenhauer, et al. 2018. "Synthesizing Models Useful for Ecohydrology and Ecohydraulic Approaches: An Emphasis on Integrating Models to Address Complex Research Questions." *Ecohydrology* 11, no. 7: e1966.

Carter, J. G., A. Karvonen, and A. Winter. 2024. "Towards Catchment Scale Natural Flood Management: Developing Evidence, Funding and Governance Approaches." *Environmental Policy and Governance* 34, no. 6: 553–567.

Chow, V. T. 1959. Open Channel Hydraulics. McGraw-Hill.

COSMOS-UK. 2020. "Monthly Summary of UK Soil Moisture Status—Archive of Monthly Summaries." Accessed July 6, 2023. https://cosmos.ceh.ac.uk/archive-monthly-summaries.

Curran, J. H., and E. E. Wohl. 2003. "Large Woody Debris and Flow Resistance in Step-Pool Channels, Cascade Range, Washington." *Geomorphology* 51, no. 1–3: 141–157.

Dadson, S. J., J. W. Hall, A. Murgatroyd, et al. 2017. "A Restatement of the Natural Science Evidence Concerning Catchment-Based 'Natural' Flood Management in the UK." *Proceedings of the Royal Society A—Mathematical Physical and Engineering Sciences* 473, no. 2199: 20160706.

de Fondeville, R., and A. C. Davison. 2022. "Functional Peaks-Over-Threshold Analysis." *Journal of the Royal Statistical Society, Series B: Statistical Methodology* 84, no. 4: 1392–1422.

Deasy, C., R. E. Brazier, A. L. Heathwaite, and R. Hodgkinson. 2009. "Pathways of Runoff and Sediment Transfer in Small Agricultural Catchments." *Hydrological Processes* 23, no. 9: 1349–1358.

Dixon, S. J., D. A. Sear, N. A. Odoni, T. Sykes, and S. N. Lane. 2016. "The Effects of River Restoration on Catchment Scale Flood Risk and Flood Hydrology." *Earth Surface Processes and Landforms* 41, no. 7: 997–1008.

Environment Agency. 2022. "Real-Time Flood Data River Flow." Accessed March 27, 2022. https://environment.data.gov.uk/dataset/8c54a361-d465-11e4-9e07-f0def148f590.

Environment Agency. 2024a. "WWNP Wider Catchment Woodland Potential." Accessed June 25, 2024. https://www.data.gov.uk/dataset/abe0c86f-4088-4d3a-8517-c6e70e2a57a3/wwnp-wider-catchment-woodland-potential.

Environment Agency. 2024b. "Oblique Aerial Photography." Accessed June 25, 2024. https://www.data.gov.uk/dataset/7f0b7c18-627b-420f-9227-5cf8ac82a905/oblique-aerial-photography.

Environment Agency. 2024c. "Historic Flood Map." Accessed June 25, 2024. https://www.data.gov.uk/dataset/76292bec-7d8b-43e8-9c98-02734fd89c81/historic-flood-map1.

Ferguson, C., and R. Fenner. 2020. "Evaluating the Effectiveness of Catchment-Scale Approaches in Mitigating Urban Surface Water Flooding." *Philosophical Transactions of the Royal Society A* 378, no. 2168: 20190203.

Ferreira, C. S. S., S. Mourato, M. Kasanin-Grubin, A. J. D. Ferreira, G. Destouni, and Z. Kalantari. 2020. "Effectiveness of Nature-Based Solutions in Mitigating Flood Hazard in a Mediterranean Peri-Urban Catchment." *Water* 12, no. 10: 2893.

Follett, E., and B. Hankin. 2022. "Investigation of Effect of Logjam Series for Varying Channel and Barrier Physical Properties Using a Sparse Input Data 1D Network Model." *Environmental Modelling & Software* 158: 105543.

Follett, E., I. Schalko, and H. Nepf. 2021. "Logjams With a Lower Gap: Backwater Rise and Flow Distribution Beneath and Through Logjam Predicted by Two-Box Momentum Balance." *Geophysical Research Letters* 48, no. 16: e2021GL094279.

Follett, E., K. Beven, B. Hankin, D. Mindham, and N. Chappell. 2024. "The Importance of Retention Times in Natural Flood Management Interventions." *Proceedings of IAHS* 385: 197–201.

Gao, J., J. Holden, and M. Kirkby. 2015. "A Distributed TOPMODEL for Modelling Impacts of Land-Cover Change on River Flow in Upland Peatland Catchments." *Hydrological Processes* 29, no. 13: 2867–2879.

Gao, J., J. Holden, and M. Kirkby. 2016. "The Impact of Land-Cover Changes on Flood Peaks in Peatland Basins." *Water Resources Research* 52, no. 5: 3477–3492.

Gao, J., J. Holden, and M. Kirkby. 2017. "Modelling Impacts of Agricultural Practice on Flood Peaks in Upland Catchments: An Application of the Distributed TOPMODEL." *Hydrological Processes* 31, no. 23: 4206–4216.

Goudarzi, S., D. G. Milledge, J. Holden, et al. 2021. "Blanket Peat Restoration: Numerical Study of the Underlying Processes Delivering Natural Flood Management Benefits." *Water Resources Research* 57, no. 4: 25

Goudarzi, S., D. Milledge, J. Holden, et al. 2024. "Natural Flood Management Through Peatland Restoration: Catchment-Scale Modeling of Past and Future Scenarios in Glossop." *Water Resources Research* 60, no. 8: e2024WR037320.

Grabowski, R. C., A. M. Gurnell, L. Burgess-Gamble, et al. 2019. "The Current State of the Use of Large Wood in River Restoration and Management." *Water and Environment Journal* 33, no. 3: 366–377.

Hankin, B., I. Hewitt, G. Sander, et al. 2020. "A Risk-Based Network Analysis of Distributed In-Stream Leaky Barriers for Flood Risk Management." *Natural Hazards and Earth System Sciences* 20, no. 10: 2567–2584.

Hankin, B., P. Metcalfe, K. Beven, and N. A. Chappell. 2019. "Integration of Hillslope Hydrology and 2D Hydraulic Modelling for Natural Flood Management." *Hydrology Research* 50, no. 6: 1535–1548.

Hankin, B., T. Page, G. McShane, et al. 2021. "How Can We Plan Resilient Systems of Nature-Based Mitigation Measures in Larger Catchments for Flood Risk Reduction Now and in the Future?" *Water Security* 13: 100091.

Hill, B., Q. Liang, L. Bosher, H. Chen, and A. Nicholson. 2023. "A Systematic Review of Natural Flood Management Modelling: Approaches, Limitations, and Potential Solutions." *Journal of Flood Risk Management* 16, no. 3: e12899.

Hundecha, Y., and A. Bárdossy. 2004. "Modeling of the Effect of Land Use Changes on the Runoff Generation of a River Basin Through Parameter Regionalization of a Watershed Model." *Journal of Hydrology* 292, no. 1–4: 281–295. https://doi.org/10.1016/j.jhydrol.2004.01.002.

Iacob, O., J. S. Rowan, I. Brown, and C. Ellis. 2014. "Evaluating Wider Benefits of Natural Flood Management Strategies: An Ecosystem-Based Adaptation Perspective." *Hydrology Research* 45, no. 6: 774–787.

Jacobs. 2022a. "Flood Modeller How to: 2D Modelling." Accessed June 23, 2024. https://help.floodmodeller.com/docs/2d-modelling-overview.

Jacobs. 2022b. "The 2D ADI Solver." Accessed June 23, 2024. https://help.floodmodeller.com/docs/the-2d-adi-solver.

Jacobs. 2022c. "Flood Modeller Technical Reference: 1D River Nodes Reference." Accessed June 23, 2024. https://help.floodmodeller.com/docs/orifice#general.

Kay, A. L., G. H. Old, V. A. Bell, H. N. Davies, and E. J. Trill. 2019. "An Assessment of the Potential for Natural Flood Management to Offset Climate Change Impacts." *Environmental Research Letters* 14, no. 4: 044017.

Keys, T., H. Govenor, C. Jones, W. Hession, E. Hester, and D. Scott. 2018. "Effects of Large Wood on Floodplain Connectivity in a Headwater Mid-Atlantic Stream." *Ecological Engineering* 118: 134–142. Kingsbury-Smith, L., T. Willis, M. Smith, et al. 2023. "Evaluating the Effectiveness of Land Use Management as a Natural Flood Management Intervention in Reducing the Impact of Flooding for an Upland Catchment." *Hydrological Processes* 37, no. 4: e14863.

Kitts, D. R. 2010. "The Hydraulic and Hydrological Performance of Large Wood Accumulation in a Low-Order Forest Stream." PhD thesis, University of Southampton.

Lalonde, M., F. Drenkhan, P. Rau, J. R. Baiker, and W. Buytaert. 2024. "Scientific Evidence of the Hydrological Impacts of Nature-Based Solutions at the Catchment Scale." *WIREs Water* 11, no. 5: e1744.

LandIS. 2016. National Soil Map of England and Wales—NATMAP. Dataset. Cranfield University. https://www.landis.org.uk/.

Lane, S. N. 2017. "Natural Flood Management." WIREs Water 4, no. 3: e1211.

Leadbetter, M. R. 1991. "On a Basis for 'Peaks Over Threshold' Modelling." *Statistics & Probability Letters* 12, no. 4: 357–362.

Leakey, S., C. J. M. Hewett, V. Glenis, and P. F. Quinn. 2020. "Modelling the Impact of Leaky Barriers With a 1D Godunov-Type Scheme for the Shallow Water Equations." *Water* 12, no. 2: 371.

Lockwood, T., J. Freer, K. Michaelides, R. E. Brazier, and G. Coxon. 2022. "Assessing the Efficacy of Offline Water Storage Ponds for Natural Flood Management." *Hydrological Processes* 36, no. 6: e14618.

Marshall, M. R., C. E. Ballard, Z. L. Frogbrook, et al. 2014. "The Impact of Rural Land Management Changes on Soil Hydraulic Properties and Runoff Processes: Results From Experimental Plots in Upland UK." *Hydrological Processes* 28, no. 4: 2617–2629.

Met Office. 2024. "UK Climate Averages." Accessed September 18, 2024. www.metoffice.gov.uk/public/weather/climate/.

Metcalfe, P., K. Beven, B. Hankin, and R. Lamb. 2017. "A Modelling Framework for Evaluation of the Hydrological Impacts of Nature-Based Approaches to Flood Risk Management, With Application to In-Channel Interventions Across a 29-km² Scale Catchment in the United Kingdom." *Hydrological Processes* 31, no. 9: 1734–1748.

Metcalfe, P., K. Beven, B. Hankin, and R. Lamb. 2018. "A New Method, With Application, for Analysis of the Impacts on Flood Risk of Widely Distributed Enhanced Hillslope Storage." *Hydrology and Earth System Sciences* 22, no. 4: 2589–2605.

Monger, F., D. V. Spracklen, M. J. Kirkby, and T. Willis. 2024. "Investigating the Impact of Woodland Placement and Percentage Cover on Flood Peaks in an Upland Catchment Using Spatially Distributed TOPMODEL." *Journal of Flood Risk Management* 17, no. 2: e12977.

Monger, F., S. Bond, D. V. Spracklen, and M. J. Kirkby. 2022. "Overland Flow Velocity and Soil Properties in Established Semi-Natural Woodland and Wood Pasture in an Upland Catchment." *Hydrological Processes* 36, no. 4: e14567.

Murphy, T. R., M. E. Hanley, J. S. Ellis, and P. H. Lunt. 2020. "Native Woodland Establishment Improves Soil Hydrological Functioning in UK Upland Pastoral Catchments." *Land Degradation & Development* 32, no. 2: 1034–1045.

Nation River Flow Archive. 2024. "27028—Aire at Armley: Peak Flow Data." https://nrfa.ceh.ac.uk/data/station/peakflow/27028. Accessed 6 July, 2023.

Nicholson, A. R., G. M. O'Donnell, M. E. Wilkinson, and P. F. Quinn. 2020. "The Potential of Runoff Attenuation Features as a Natural Flood Management Approach." *Journal of Flood Risk Management* 13: e12565.

Norbury, M., H. Phillips, N. Macdonald, et al. 2021. "Quantifying the Hydrological Implications of Pre- and Post-Installation Willowed Engineered Log Jams in the Pennine Uplands, NW England." *Journal of Hydrology* 603: 126855.

Ordnance Survey. 2022. "Terrain 5 [ASC Geospatial Data], Scale 1:10000, Updated: 13 November 2021, Ordnance Survey (GB), Using:

EDINA Digimap Ordnance Survey Service." March 25, 2022. https://digimap.edina.ac.uk.

Pattison, I., S. N. Lane, R. J. Hardy, and S. M. Reaney. 2014. "The Role of Tributary Relative Timing and Sequencing in Controlling Large Floods." *Water Resources Research* 50: 5444–5458.

Pinos, J., and L. Timbe. 2019. "Performance Assessment of Two-Dimensional Hydraulic Models for Generation of Flood Inundation Maps in Mountain River Basins." *Water Science and Engineering* 12, no. 1: 11–18.

Ramsbottom, D., A. Pinto, M. Roca, and R. Body. 2019. "Effectiveness of Natural Flood Management Measures." In *Proceeding of the 38th IAHR World Congress*, edited by L. Calvo. International Association for Hydro-Environment Engineering and Research (IAHR).

Rowland, C. S., R. D. Morton, L. Carrasco, G. McShane, A. W. O'Neil, and C. M. Wood. 2017. "Land Cover Map 2015 (Vector, GB)." Dataset. NERC Environmental Information Data Centre. https://doi.org/10.5285/6c6c9203-7333-4d96-88ab-78925e7a4e73.

Senior, J. G., M. A. Trigg, and T. Willis. 2022. "Physical Representation of Hillslope Leaky Barriers in 2D Hydraulic Models: A Case Study From the Calder Valley." *Journal of Flood Risk Management* 15, no. 3: e12821.

Shen, Y., Z. Xu, Q. Zhou, Z. Zhu, and C. Jiang. 2024. "A Direct Two-Way Coupling of the Hydrologic and 1D-2D Hydrodynamic Models for Watershed Flood Simulation." *Journal of Hydrology* 639: 131606.

Shields, F. D., and C. V. Alonso. 2012. "Assessment of Flow Forces on Large Wood in Rivers." *Water Resources Research* 48, no. 4: W04516.

Shuttleworth, E. L., M. G. Evans, M. Pilkington, et al. 2019. "Restoration of Blanket Peat Moorland Delays Stormflow From Hillslopes and Reduces Peak Discharge." *Journal of Hydrology X* 2: 100006.

Stamataki, I., and T. R. Kjeldsen. 2021. "Reconstructing the Peak Flow of Historical Flood Events Using a Hydraulic Model: The City of Bath, United Kingdom." *Journal of Flood Risk Management* 14: e12719.

Strahler, A. 1957. "Quantitative Analysis of Watershed Geomorphology." Transactions of the American Geophysical Union 38, no. 6: 913–920.

Thaler, T., P. Hudson, C. Viavattene, and C. Green. 2023. "Natural Flood Management: Opportunities to Implement Nature-Based Solutions on Privately Owned Land." *WIREs Water* 10, no. 3: e1637.

Thomas, H., and T. Nisbet. 2012. "Modelling the Hydraulic Impact of Reintroducing Large Woody Debris Into Watercourses." *Journal of Flood Risk Management* 5, no. 2: 164–174.

Turcotte, B., R. G. Millar, and M. A. Hassan. 2015. "Drag Forces on Large Cylinders." *River Research and Applications* 32, no. 3: 411–417.

UKCEH. 2012–2020. "Monthly Hydrological Summaries." Accessed July 6, 2023. https://nrfa.ceh.ac.uk/monthly-hydrological-summary-uk.

UKCEH. 2015. "UKCEH Land Cover Maps." Accessed May 17, 2023. https://www.ceh.ac.uk/data/ukceh-land-cover-maps.

van Leeuwen, Z. R., M. J. Klaar, M. W. Smith, and L. E. Brown. 2024. "Quantifying the Natural Flood Management Potential of Leaky Dams in Upland Catchments, Part II: Leaky Dam Impacts on Flood Peak Magnitude." *Journal of Hydrology* 628: 130449.

Villamizar, M. L., C. Stoate, J. Biggs, J. Szczur, P. Williams, and C. D. Brown. 2024. "A Model for Quantifying the Effectiveness of Leaky Barriers as a Flood Mitigation Intervention in an Agricultural Landscape." *River Research and Applications* 40, no. 3: 365–378.

Wilcox, A. C., and E. E. Wohl. 2006. "Flow Resistance Dynamics in Step-Pool Stream Channels: 1. Large Woody Debris and Controls on Total Resistance." *Water Resources Research* 42, no. 5: W05418.

Wilkinson, M. E., S. Addy, P. F. Quinn, and M. Stutter. 2019. "Natural Flood Management: Small-Scale Progress and Larger-Scale Challenges." *Scottish Geographical Journal* 135, no. 1–2: 23–32.

Xiao, L., M. Robinson, and M. O'Connor. 2022. "Woodland's Role in Natural Flood Management: Evidence From Catchment Studies in Britain and Ireland." *Science of the Total Environment* 813: 151877.

Yorkshire Wildlife Trust. 2022. *Upper Aire Catchment: NFM Projects*. Yorkshire Wildlife Trust.

Zhu, Q., M. Klaar, T. Willis, and J. Holden. 2024. "A Quantitative Review of Natural Flood Management Research." WIREs Water 12: e1765.

Zhu, Q., M. Klaar, T. Willis, and J. Holden. 2025. "Use of Spatially Distributed TOPMODEL to Assess Effectiveness of Diverse Natural Flood Management Techniques for a UK Catchment." *Hydrological Processes* 39: e70122.

Supporting Information

Additional supporting information can be found online in the Supporting Information section. **Data S1:** Supporting Information: Figures to demonstrate the point-to-point coupling method. **Data S2:** Supporting Information: Figures to demonstrate model validation, wider catchment woodland scenario and full hydrograph outputs. **Data S3:** Supporting Information: Table to explain the goodness-of-fit metrics and their associated attribute.